Atomic Quantum Memory for Photon Polarization

by

Benjamin Jacob Bloom

Submitted to the Department of Physics
in partial fulfillment of the requirements for the degree of

Bachelor of Science in Physics

at the

MASSACHUSETTS INSTITUTE OF TECHNOLOGY

June 2008

Author .....
Department of Physics
May 16, 2008

Certified by .....
Vladan Vuletić
Lester Wolfe Associate Professor of Physics
Thesis Supervisor

Accepted by .....
David E. Pritchard
Cecil and Ida Green Professor of Physics, Senior Thesis Coordinator

Atomic Quantum Memory for Photon Polarization

by

Benjamin Jacob Bloom

Submitted to the Department of Physics
on May 16, 2008, in partial fulfillment of the
requirements for the degree of
Bachelor of Science in Physics

Abstract

Using an ensemble of ultracold Cesium atoms in an optical cavity we demonstrate the efficient storage and retrieval of quantum information in the form of single photons. We use a photon that has scattered into the cavity mode to herald a successful creation of a collective excitation of Cesium atoms and hence our ability to retrieve a photon from the stored excitation at a later time. Post-selecting out only data that was preceded by a heralding photon we have achieved single-photon recovery efficiencies as high as 84%. We construct an atomic quantum memory for arbitrary optical polarization states using this technique on two spatially overlapped atomic samples. The two samples constitute a quantum memory making use of a bijective mapping between a photon polarization and a shared collective excitation in the atoms. The stored state is later retrieved as a single-photon polarization state. This memory showed an average fidelity of 0.93(5) for the recovered fiducial states as well as a conditional autocorrelation function $g_2 = 0.24(6)$, indicating the single-photon nature of the retrieved photons. In this thesis, a general discussion of the techniques employed and their background theory will be given, followed by a more detailed explanation of this most recent experiment.

Thesis Supervisor: Vladan Vuletić
Title: Lester Wolfe Associate Professor of Physics

Acknowledgments

The existence of this thesis is thanks in no small part to the help of four amazingly inspiring and brilliant physicists: Jonathan Simon, Haruka Tanji, Saikat Ghosh, and Vladan Vuletic. It is because of their amazing ingenuity and dedication to the pursuit of knowledge that an experiment as complicated as ours is ever successful. Because of their guidance and mentoring, I am a better physicist today than I would ever have been otherwise. My most sincere thanks go to Jon, who not only read the first draft of this text, but who has again and again in the last year and a half answered all the questions I have confronted him with. Jon has helped me to understand both the qualitative and quantitative aspect of every possible physical process in our experiment, and offers immense insight into the issues of atomic physics. While Jon's characteristic mode to work is to plunge forward with it, Haruka's careful examination of the fundamentals of every problem is a calming influence in the lab that leads to clever answers to difficult problems and a voice of reason in all physics discussions. Saikat, the postdoc, exhibits the wonder that I associate with those who push the frontiers of scientific research. Knowledgeable over the entire breadth of physics, he is a constant source of excitement in the lab as he can connect what seems like mundane, ordinary labwork to much larger principles that guide current research in a variety of fields. I cannot thank Jon, Haruka, and Saikat enough for not only their help in preparing this thesis, but for their friendship over the last year and a half. Regardless of how far away I am in the future, I hope that I will always be able to call them *my friends*.

I would also like to acknowledge Vladan who exhibits every quality of a truly-brilliant physicist. A wealth of ideas and insight, every time Vladan steps into lab to discuss either our experiment or a new paper everybody drops whatever it is they are doing to hear everything he has to say. Pushing the boundaries of quantum mechanics, Vladan seems to me to be the Sherlock Holmes of Atomic physics, never without a trick up his sleeve or the most logical explanation at his disposal. He is an inspiration to me and to the rest of the lab.

But looking beyond the lab, first and foremost, I would like to thank my parents for supporting me in every way throughout the last four years. This thesis represents my long journey through MIT, and as such I want to thank a number of people who have helped me in other projects and classes I have worked on throughout my four years here. Whether it was slogging through problem sets, performing analysis on the latest Junior Lab experiment, or heeding the call of Lobster Bisque during a blizzard, William McGehee, my old JLab partner, has been an incredible friend to me and I do not know if there is any way I will ever be able to repay him. Similarly, Ruth Shewmon and Elizabeth George, the other CUA UROPS, were an immeasurable source of strength in that our shared suffering always allowed me to continue working hard. The same goes for all of the other brilliant graduate students and UROPS at the CUA who helped me along the way, especially Marko Cetina, Andrew Grier, Ian Leroux, and Monika Schleier-Smith. And last but not least at the CUA, the amazing Ketterle coffee machine.

Outside of Atomic physics, I would like to thank all of those that have helped me through my classes: Grant Elliott, Louis Fernandes, Shawn Henderson, Alan Dibos, Asher Kaboth, Daniel Furse, James Hays-Wehle, Christopher Jones, Nicole Ackerman, Anjan Soumyanarayanan, and Tran the enigmatic Physics Reading room guy. And finally I want to thank all my other friends not in physics, without their company and camaraderie I would not at this moment be warmly remembering the time I have spent here at MIT.

Contents

List of Figures

List of Tables

Chapter 1

Introduction

In a flash of brilliance, Richard Feynmann proposed the use of a quantum system as a means for computational processing, an idea that has yet to be demonstrated on a large scale. By utilizing the massively parallel properties inherent in working in a direct product space, one is able to perform calculations that were previously considered intractable in a finite amount of time. Subsequently, it was realized that quantum mechanics was the key to creating secure communications protocols between disparate parties as the effect an observer has on a quantum system could be used to identify whether an eavesdropper existed on the communication channel. But what is the fundamental unit that people could calculate with or could send to each other in communication protocols? The answer is a new kind of information: Quantum Information. This new form of information cannot be approximated by classical quantities and cannot be reproduced once it has been lost, or decohered. The relevant quantum information for any given experiment might be an overlap of two wave functions, a phase relationship between two states, or maybe the degree of entanglement between two variables.

The storage of quantum information is key to the building of Quantum Networks and Quantum Computing experiments. A quantum network is defined as a set of interconnected nodes with the ability to pass information from one node to the next without degradation of the information [14]. Large scale quantum communication would only be possible if we had some means to implement such a network. A key

component in analog networks is the buffer or memory which holds the information while whatever transfer protocol between two nodes is being initialized. Without a reliable means of storing quantum information for periods of time longer than the time required for the initialization, any attempts to facilitate synchronization between two disparate nodes in a quantum network would be arduous and any hopes of realizing a large scale secure quantum communications network would be destroyed. Similarly, quantum computation schemes which involve interactions between many particles need a buffer to facilitate the propagation of information from one part of the system to the system's entirety. But how are we to implement such a buffer, and of what material should it be constructed?

The most important quantity we must analyze when evaluating what the quantum memory should be constructed from is the time scale of possible storage. At first sight, photons might seem like the best candidate as we may encode quantum information in them, but the trapping of photons for long times is extremely difficult [16]. However, photons stand in the fortuitous intersection between information carriers and information translators to and from matter. Therefore, the atoms they strongly interact with are the perfect medium to build a quantum memory. On this basis, we demonstrate the use of an ensemble of atoms as a storage medium with decoherence times in the tens of microseconds. With long decoherence times and low signal degradation our system performance makes our implementation competitive to the other proposed mechanisms for the storage of quantum information [7, 6, 21].

In particular, we utilize collective excitations of Cesium atoms, known as spin-waves or magnons, derived from a weak coherent beam to construct a quantum memory [40]. The read out of the memory is accomplished by the generation of a single photon that carries the original polarization state. Our procedure uses a low finesse cavity with many atoms to achieve strong atom-photon coupling without excessive technical difficulties [2, 4, 39, 3, 27]. By optically pumping two samples of Cesium atoms we are able to restrict the allowed atomic transitions to a small subset of states to perform our experiment in. Furthermore, using a heralding scheme, the dynamics of the system can be simplified to effectively mimic two 3-level systems. This sys-

tem can be modeled using a combination of creation and annihilation operators in both the photon number space and the atomic energy space, formally known as a Jaynes-Cumming model. One important difference from generic models remains as these operators describe collective excitations shared across many atoms rather than single-atom excitations. By taking advantage of the heralding process we are able to store an optical polarization state and retrieve it in the form of a single-photon with a high-fidelity of input state regeneration.

Thermal motion of the atoms is one of the major causes of decoherence and as such must be minimized at all cost. To this effect we laser cool and trap the Cesium atoms in a Magneto-Optical Trap (MOT) as illustrated in Figure 1-1. Once the atoms are confined in space, they are further cooled by Polarization Gradient Cooling to temperatures below the Doppler limit. The entire sample is then optically pumped into two states. The separation into two states allows us to map the two degrees of freedom of the optical polarization state to those of the atoms, thereby achieving a bijective mapping of information in the storage process. To facilitate phase matching a homogeneous magnetic field is applied across the atoms and the samples' magnetic moment precesses about the field. Examining one sample, and knowing that the other sample behaves in much the same way, we will see how a collective excitation is created and retrieved. A beam, which we call the *Write* beam, is briefly sent into the sample to induce a transition of one of the atoms from the ensemble prepared in the ground state to an excited state, $|e\rangle$. This excitation quickly decays into a third state emitting a photon along the way. Should this photon be emitted into the cavity mode and be detected, it acts as a flag that the sample has been prepared with one collective excitation. As each atom in this collection of atoms has a chance of being the excited atom, a superposition state known as a Dicke state has been created. Driving the system with a phase matched *Read* beam induces transitions back into the ground state with the concomitant emission of a photon.

What makes this scheme viable is the collective enhancement, known as superradiance, seen in the last process compared to the free space emission of photons by the factor, $N\eta$, the effective optical depth of the sample in the optical cavity. As the *Read*

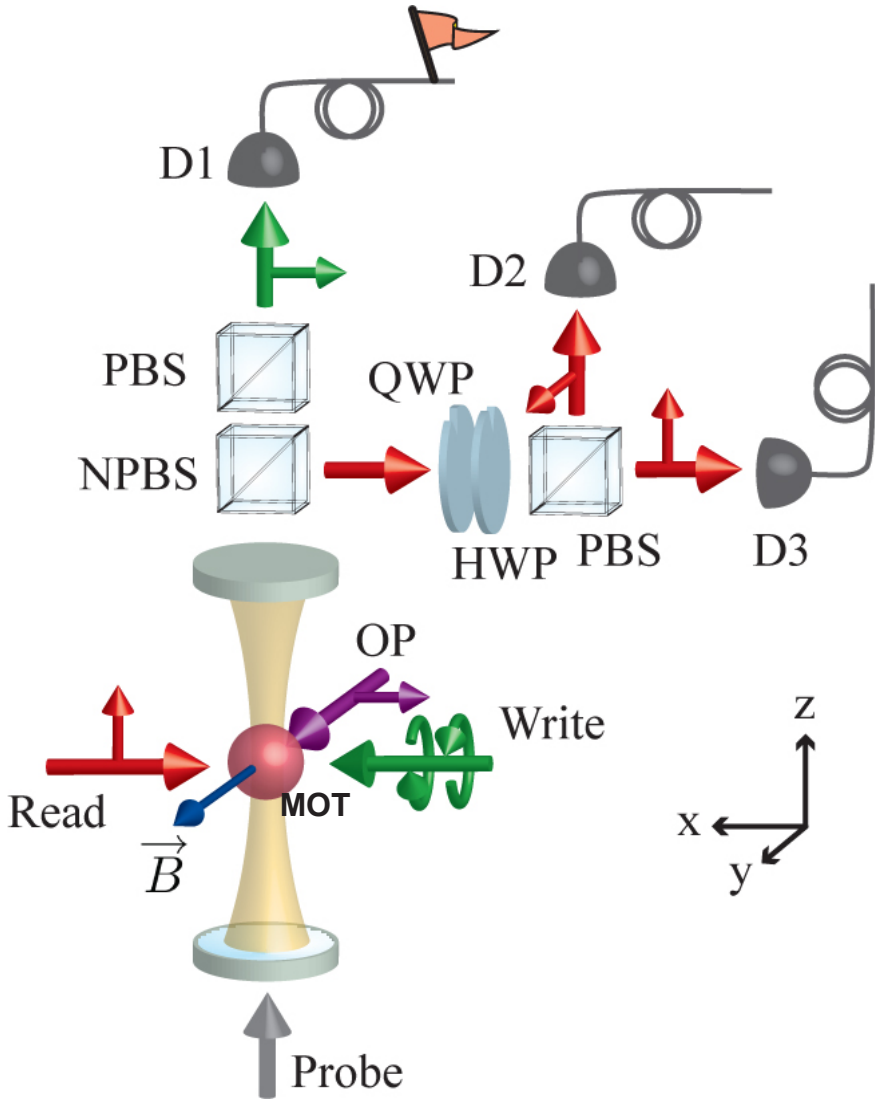

Figure 1-1: An illustrated overview of the entire experiment. A sample of ultracold Cesium atoms in an optical cavity stores the polarization state of the *Write* beam to be later ejected from the cavity into the polarization analyzation equipment on top of the resonator. The output of the polarization analyzation coupled with our knowledge of what the state to be stored actually is allows us to calculate what fidelity we see in the storage of quantum information[42]

.

beam travels through the sample, superradiance corresponds to the sample becoming opaque to the beam as the probability of scattering into the cavity, η is enhanced by every atom. To control what we store in the system we can vary the *Write* beam's polarization state which generates entanglement between the two optically pumped samples according to the state by a bijective mapping of input polarization to atomic entanglement and then to the output photon polarization. As we can control when the output photon leaves the sample, in essence we have implemented a single-qubit quantum memory.

In this thesis, all aspects of the design and implementation of this quantum memory will be explained starting from first principles. While all the pieces of this experiment together form an intricate web, if we analyze each piece individually we can identify common themes in their operation. By starting with simple techniques and building up to sophisticated methods widely employed in cold atom experiments, the complicated behavior of our system will become analytically tractable. Once some of the methods at our disposal have been explained we will move on to a discussion of the theory behind the preparation of a cold atomic sample. We will then discuss how we implement our heralding scheme for single photon generation and subsequently how we can modify the scheme to be used as a polarization state storage device. Finally, results will be given from our experiment and a cursory examination of further extensions of this experiment will be discussed in the conclusion.

Chapter 2

Preparation of Laser Cooled Atoms

2.1 Lasers

Since the initial conception of a coherent source of microwaves created by population inversion and stimulated emission, no technology created by physicists has influenced as wide a variety of fields as communications [22], data storage [20], and medicine [1] as has the modern Laser [35]. Accounting for the broad range of applications that the laser lends itself to, it is easy to forget the purpose it serves in an atomic physics lab: a precise means of exciting narrow transitions between energy levels in atoms. Were it not for the exquisite control we have over the the frequency of the lasers used and their narrow linewidth, the manipulations performed in this experiment on thhe collection of Cesium atoms would be impossible. Lasers allow us to efficiently address extremely narrow transitions to a degree of accuracy that allows us to see the doppler the shift caused by a Cesium atom moving $1\ \frac{\text{cm}}{\text{s}}$. To explain how such control is achieved a brief introduction to lasers is given in Section 2.1.1 followed by a discussion of how a laser's frequency is controlled in Section 2.1.2 and a brief description of the other rlevant instruments we use to control both a laser's frequency and its trajectory during the experiment in Section 2.1.3.

2.1.1 Distributed Feedback Lasers

The concept of a maser or a laser is rather simple and can be explained in the language of quantum mechanics with relative ease. Quantum mechanically one can envision creating a laser by utilizing a 3 level system found in Figure 2-1. For ease of reference we will label these states $|0\rangle$, $|1\rangle$, and $|2\rangle$ labeled the ground, middle, and highest energy states respectively. In this example we will require that $|2\rangle$ has a short lifetime and there is nothing prohibiting it from decaying to $|1\rangle$. In the case of the early masers one would place whatever atomic vapor exhibits this energy structure in a standing wave cavity resonant with the $|1\rangle$ to $|0\rangle$ transition and set up a pumping mechanism, an oscillating electric field, that would bring electrons up from $|0\rangle$ to $|2\rangle$. These electrons would quickly fall down to $|1\rangle$. At the beginning of the sequence spontaneous emission would bring them down to the ground state but eventually the photons created by this transition, having been trapped inside the cavity, will cause stimulated emission of even more cavity resonant photons bringing the electrons back to the ground state only to be repumped and start the process again [28]. As one can see this creates a process by which more and more photons will be created until an equilibrium is achieved between photon creation and photon leakage out of the cavity. This equilibrium is caused by a non-linearity in photon creation. The existence of state $|2\rangle$ is imperative in this setup as Einstein's absorption and stimulated emission coefficients being equal prohibits any two level scheme from creating some kind of self sustaining photon creation reaction.

Schawlow and Townes insight into extending this technique towards smaller and smaller wavelength photon sources leads perfectly into a more classical description of the laser in terms of waves instead of photons which we will use to cross the gap from vapor lasers to semiconductor lasers, specifically Distributed Feedback lasers (DFB). With the inability to manufacture extremely small cavities useful as standing wave cavities the transition to lasers was facilitated by designing traveling wave cavities that would ensure constructive interference for the specific wavelength of light that was being created [35]. With this in mind a better description of the laser, in classical

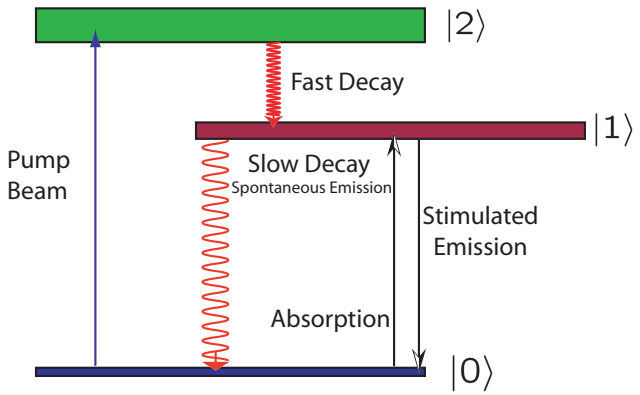

Figure 2-1: A three level system to demonstrate the concept of population inversion, especially how it is employed in the construction of lasers.

terms, is called for. One can picture a cavity whose center is filled with some kind of material which we will call a Gain Medium which enhances the amplitude of the field by a minuscule amount. Assuming the plane wave is resonant with the cavity each time it bounces from one mirror to the next it will travel through this gain medium once. However small the gain medium's addition to the amplitude of the field is, if the plane wave bounces around in the cavity many times and has an overall gain greater than the loss through the cavity mirrors, these amplifications will add up and just like the equilibrium reached when we were discussing discrete photons a new equilibrium will be reached in which the light that leaks out of the cavity will be replenished by a single trip through the gain medium [28].

Diode lasers are made from light-emitting PIN junctions, light being created by the recombination of electron hole pairs. The so-called grating lasers that are widely employed throughout the physical sciences pick off the light from these diodes in a wavelength specific way by carefully orienting a reflective grating onto a mirror. In this way choice of the wavelength is made by simply rotating the grating. The cavity formed between the grating and the diode, even though it has a low finesse (tge number of times light bounces back and forth inside the optical resonator) narrows the laser to less than a megahertz. Two scales of frequency control are left to us. First, a coarse control by heating or cooling the laser package which controls the length of the cavity. Second, a more precise control of the frequency based on the current supplied

to the diode. However, rather than grating-laser diodes, in this experiment we almost exclusively use DFB laser diodes. These diodes collect the light they emit and send it into a material with a modulated index of refraction as in Equation (2.1) [23].

$$n(z) = n + n_1 cos(2\beta_0 z) \tag{2.1}$$

Where β_0 is a measure of the periodicity of the refractive index in the medium. Similar to the traveling wave interpretation of laser cavities we can imagine that as the light travels through this medium, only waves that are at or near the perfect frequency to constructively interfere with back reflected waves just like a cavity make it through, Figure 2-2. The linewidth for these semiconductor lasers is also quite small: for example, we have a linewidth of 2 MHz for the 852 nm diodes that we purchased from Eagleyard Photonics [15]. There are many causes for the broadening of frequency. The largest contributor in semiconductor lasers is the change in the refractive index of the diode itself as electron-hole carrier density in the PIN junction fluctuates [18]. Now that we have succeeded in creating narrow sources of coherent light we will move on to how we manipulate them for use in this experiment.

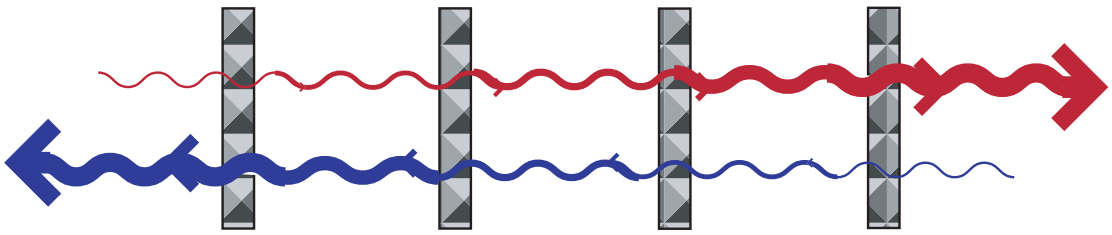

Figure 2-2: Distributed feedback lasers are constructed to have a variable index of refraction, such that only the desired wavelength of light can constructively interfere and thus be enhanced. This illustration of this principle is similar to one found in [23]

.

2.1.2 Laser Locking

The purpose of laser locking is to stabilize the frequency of the laser relative to a chosen atomic transition. While at first glance this problem might seem trivial, it is

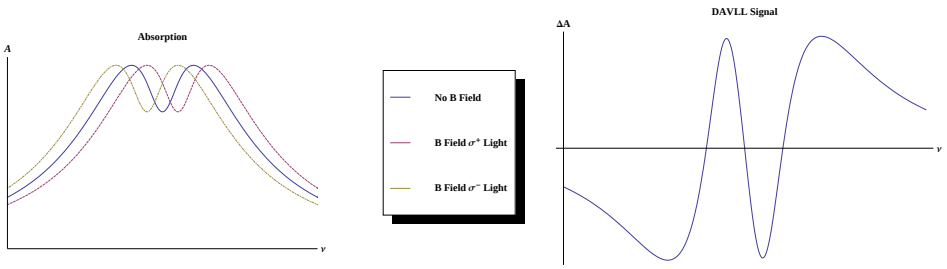

(a) (b)

Figure 2-3: (a) Due to an antisymmetric energy shift between two polarizations of light, $\sigma^{\pm}$, caused by the addition of magnetic fields, absorption signals of atomic transitions exhibit shifts dependent on which polarization of light is used to probe the sample. (b) The electronic DAVLL signal is showcased with the correct locking point being the middle crossing of zero.

in fact a complicated procedure that is repeated everyday in lab. To begin with, in this experiment there are six lasers in lab that need to be locked onto various Cesium transition frequencies. This is most easily accomplished by creating a reference laser to which all of the other lasers in the lab are locked to. As all of our experiments are performed in the fine structure or hyperfine structure of Cesium near the 852 nm D_2 line the reference must be locked to this line. This allows us to address different transitions by locking the other lasers to the reference using beatnote signals.

It should be apparent to the reader that with present technology we cannot create stable signals on the order of terahertzs to lock to and the best way to lock a laser to a specific Cesium electron transition is to use a separate carefully controlled sample of Cesium atoms in a vapor cell to act as our "source" for the frequency. While these atoms will exhibit the same electron structure as those found in the chamber, effects such as doppler broadening of the transition lines and power drift of the reference laser must be corrected for. Many different approaches to locking a laser to a vapor cell exist such as Saturated Absorption Spectroscopy, Polarization Spectroscopy, and other Sub-Doppler Spectroscopy Schemes. We utilize a Doppler-Free Dichroic Vapor Laser Lock scheme (DAVLL) to accurately lock our reference laser.

In doppler-free DAVLL the beam that is meant to be locked is sent through the vapor cell with its frequency being swept back and forth. Doppler-free DAVLL can

be separated into two distinct laser addressing processes. The Doppler-free part of the laser lock works by splitting the beam to be locked into a strong pump beam and a weak probe beam. Both beams are sent through the sample propagating in opposite directions. The pump beam saturates whatever transition it is tuned to resonance for one velocity class of atoms, while the probe beam as it is propagating the other direction will address a different velocity class of atoms corresponding to the same transition and will be absorbed. Measuring the absorption of the probe beam on the photodiode and dithering the laser frequency, there will be a huge dip in the probe beam absorption signal when it tries to address the same atoms that the pump beam has already saturated. This corresponds to the few stationary atoms in the cell. By selecting out the atoms with no doppler broadening in their frequency we have decreased the frequency broadening from its previous width on the order of 1 GHz to the 5 MHz linewidth intrinsic to the electron's coupling to free space during the atomic transitions.

The second stage of this laser lock, the DAVLL, is meant to recuperate from any broadening that might be induced by the degeneracy of nearby magnetic sublevels. Looking at the probe beam's absorption through the cell on a photodiode, as stated before the absorption will dip near the central frequency of the transition. Without a magnetic field, there is no difference in the absorption spectrum between sending in σ^+ or σ^- light. However in a DAVLL scheme, we place the sample in a uniform magnetic field which splits the magnetic sublevels which were all previously degenerate as can be seen in Figure 2-3. Paying closer attention to the transition energies we see that σ^+ transitions will now be of slightly higher frequency and σ^- transitions will be slightly lower. The most important thing to note about these shifts is that they are symmetric about the original transition frequency. Therefore if we were to send in both polarizations of light and subtract the absorption profile of one polarization from the other, the point where they were equal, i.e. the point the two spectrums diverged from will be the central frequency of the transition. As the absorption of the beam is equal at this point and we subtracted one spectrum from the other the center frequency is the point where the DAVLL signal crosses zero.

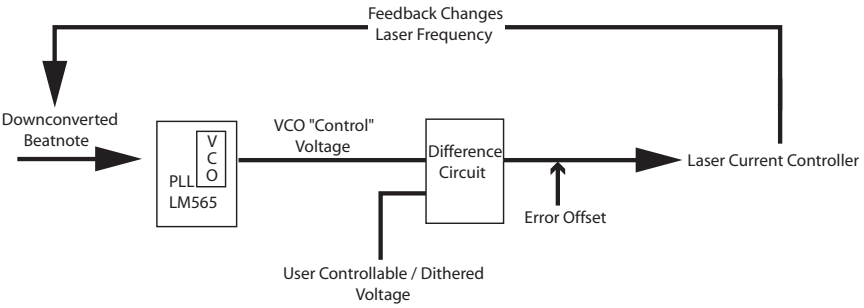

Figure 2-4: A Phase Locked Loop is used to lock one laser to another laser, in our case the Reference Laser, and is employed in most of the laser locks throughout the Vuletic lab.

Rather than send in two beams of different polarizations, linearly (lin) polarized light is sent into the vapor cell as lin polarized light can be decomposed into a superposition of both σ^+ and σ^- light. Thus the output of the vapor cell is directed through a $\frac{\lambda}{4}$ waveplate set 45° from the h-v basis and into a Polarizing Beam Splitter (PBS). This chain of optics after the vapor cell separates out the two polarizations, as if we had sent two separate beams through the cell. Both the transmitted and the reflected port of the PBS is then analyzed in the exact manner which we mentioned before, by dithering the frequency of the laser and looking at the difference of absorption spectra and locking the signal with a PI loop on the current controller for the laser. To explain how we commonly create this feedback loop on the lasers current controller we can examine how we lock other lasers to the reference laser. The MOT and the Repumper laser both use Phase Locked Loops (PLLs) as seen in Figure 2-4. Picking off some of the reference beam and, for this example, the MOT laser we spatially overlap the two on a photodiode. As photodiodes only measure intensity, the photodiode signal will be proportional to both beams' intensities plus a cross term seen in Equation (2.2).

$$I = |E_{ref}|^2 + |E_{repump}|^2 + 2E_{repump}E_{ref}\ cos(2\pi\Delta\nu) \tag{2.2}$$

Unfortunately the beatnote that we now see is on the order of GHz. The first step is to downconvert this signal by mixing in a fixed 9.2 GHz local source bringing the signal down to a few hundred MHz. To further downconvert the signal we run this

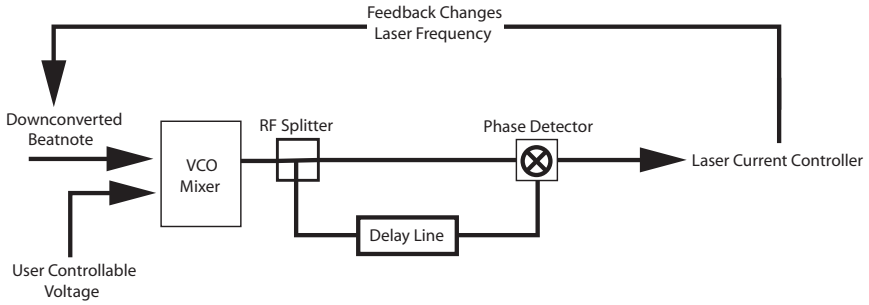

Figure 2-5: Similar to the PLL, a Delay Line Lock is used to lock one laser to another laser.

through a set of two digital counter circuits that bring the signal down to 100 KHz.

This beatnote is then sent into an LM565 phase locked loop IC that includes a Voltage Controlled Oscillator (VCO). The internal VCO locks itself to this frequency and a DC voltage derived from the VCO frequency is available on one of the pins. Next we send the VCO "control" voltage along with a user controllable voltage to a difference chip to create our error signal. Finally the output of the difference circuit, with the possible addition of a user controllable output offset, is fed to the laser current controller which creates the feedback as changes in the laser current change the laser frequency and close the feedback loop. To lock these PLLs we electronically dither the output offset back and forth; when we find the right place for the output offset the error signal is a linear response of opposite slope to the dithering. Once the output offset is exhibits this linear behavior, we flip the feedback on and the laser stays at the correct frequency. The other method employed for locking a laser with the reference laser is a Delay Line Lock (DLL). Three lasers in our system are locked with a DLL: the Eta, Gamma, and Cavity lasers. Similar to the previous method the beatnote is downconverted to a signal on the order of a 100 MHz and then mixed with a user tunable VCO. The signal is then split with an RF amplifier with one path going directly to one input of a phase detector and the other going through a delay line on the order of a meter and then into the phase detector. This phase detection loop as illustrated in Figure 2-5 creates a DC voltage that is sent into a difference circuit connected to the laser current controller just like in the PLL circuit.

To be more specific, the added phase that the beatnote sees from having gone

through a delay line, Φ, causes the phase detector to create a DC voltage according to Equation (2.3)

$$V \propto cos(\Phi) \qquad \Phi = 2\pi(\Delta\nu - \nu_{VCO})\tau \tag{2.3}$$

where $\Delta\nu$ is the difference in laser frequencies and τ is the propagation delay [36]. To lock a DLL one sets the VCO to a point where the error signal crosses zero, where it exhibits the maximum slope. A simple comparison between possible noise sources for this kind of measurement shows us that we are in fact photon shot noise limited when we assume that total power on the photodiode, the sum of the power for the reference and the laser, is much larger than the power of the laser we are trying to lock. In addition the uneven power distribution we create on the photodiode allows us to ignore the power of the reference beam in the calculation of noise, thereby not adding more noise in the measurement process than we started with, this is common to most heterodyne measurements. With such exquisite control over frequencies over long periods of time it is now time to look at techniques for performing quick manipulations to the lasers' frequency and direction.

2.1.3 Acousto-Optic Modulators and Electro-Optic Modulators

Implementing the *Write* and *Read* scheme and many of the complicated steps in the preparation of laser cooled atoms requires that we have extremely fast control of the lasers themselves during the experimental sequence. To this end we employ two different kinds of devices: Acousto-Optic Modulators (AOMs) and Electro-Optic Modulators (EOMs). Both can be used to control the power and frequency of the laser, and while the AOM works on timescales of hundreds of nanoseconds the effects of EOMs are seen in just a few nanoseconds.

First we examine AOMs as they serve two very useful purposes, by adding or subtracting a fixed frequency offset to the light and physically deflecting the light's normal trajectory. AOMs work by creating an acoustic wave propagating in the crystal medium the light is traveling through. This acoustic wave sets the crystal to

deflect the laser towards the propagation of the acoustic wave and in turn adding a frequency offset (80 or 110 MHz in the Isomet AOMs that are in our experiment) or in the antiparallel direction from the acoustic wave and in turn subtracting a frequency offset [29].

$$\begin{aligned} \omega_{scat} &= \omega \pm \Omega_{AOM} \\ k_{scat} &= k \pm \kappa_{AOM} \end{aligned} \tag{2.4}$$

The amount of light deflected is related to the power of the driving signal used to create the acoustic wave. Controlling this driving power via a computer one is able to control the amount of laser being deflected or to put it another way, the power of the beam. However due to the low velocity of the acoustic wave in the crystal, AOMs are not the fastest amplitude manipulators at our disposal.

EOMs bought from EOSpace are made from a waveguide mounted on a birefringent substrate, in this case lithium niobate. Placing an electric field across the birefringent substrate changes the phase it imparts on light polarized along the axis of the electric field. When the light traveling through the lithium niobate interferes with the light traveling through the waveguide, an effective Mach-Zehnder interferometer is created [32]. Therefore modulation of the electric field allows one to control the phase of the output wave which can be used to add a sideband to the carrier light, and in principle can be used to control the amplitude. However we do not employ this feature of EOMs in our current experiment. With all these tools in place we will now examine the process of laser cooling of the atoms.

2.2 Cooling Processes

The longevity of the magnons we create is essential to the process of heralding single photon storage or generation. If atoms in the sample move in a way that destroys the phase information created by scattering a *Write* photon, all collective effects that make this experiment possible will be destroyed. While the exact mechanism for the loss of coherence among atoms will be discussed in Section 4.2.2 suffice it to say that to perform our experiment the kinetic energy and therefore the temperature of the

Cesium atoms must be reduced. Furthermore, to better address all the atoms for storage and readout we must spatially confine them to increase their optical depth. After a brief introduction to Doppler cooling, we will discuss the construction of a magneto-optical trap (MOT) and the implementation of Polarization Gradient Cooling (PGC) in our experiment.

The first step in laser cooling atoms is localization and isolation of atoms. Our entire experiment is preformed inside an ultra high vacuum chamber kept at approximately 3×10^{-9} torr. Each time the chamber is opened, approximately once every 18-24 months, extreme care is taken to keep the inside chamber clean from any dust or oil. A lengthy bake out and pump down period follows each opening of the chamber to ensure that we can perform experiments without contamination from non Cesium particles. The first and most simple technique for laser atom cooling that will be discussed is Dopper cooling colloquially known as the application of an Optical Molasses.

2.2.1 Magneto-Optical Trap

As atoms move with respect to laser sources they observe a doppler shift to the laser frequency. This classical doppler shift of frequency is only due to the longitudinal motion of the atom along the direction of propagation of the beam and is equal to: $\vec{k} \cdot \vec{v}$. The scattering rate for a beam falling on these atoms can be found in Equation (2.5).

$$\begin{gathered} \Gamma_{sc} = \frac{P}{1+P} \frac{\Gamma}{2} \\ P = \frac{S}{1+\delta^{*2}} \quad \delta^* = \frac{\delta - \vec{k} \cdot \vec{v}}{\frac{\Gamma}{2}} \quad S = \frac{I}{I_s} \end{gathered} \tag{2.5}$$

The Raman Scattering equation above characterizes the action of a beam of photons detuned from atomic resonance by δ and with intensity $I = \frac{2P_{laser}}{\pi w^2}$ where the saturation intensity is 1.1 $\frac{mW}{cm^2}$. One might wonder how if the atom has an equal probability to scatter the photon in any direction there will be any kind of net force on the atom. Given that the incoming photons come from the same directions it is easy to see that with $\Delta p \propto k_f - k_i$ averaging over many scattering events sends $\langle k_f \rangle$ to zero while

$\langle \Delta p \rangle \propto k_i$. This implies that the longitudinal motion of atoms along the direction of propagation of a light source can be damped.

To create a trap that damps the motion of our Cesium atoms in all directions we use three perpendicular circularly polarized beams that are each retroreflected through $\frac{\lambda}{4}$ waveplates. When aligned, the intersection between all six beams damps the motion of our atoms in all three dimensions. Working with the beams tuned to the red of the $\left|6^2S_{\frac{1}{2}}, F = 4\right\rangle$ to $\left|6^2P_{\frac{3}{2}}, F = 5\right\rangle$ transition, this closed transition works well for laser cooling, however it is still possible to off-resonantly excite an $F = 4$ to $F' = 4'$ transition which decays down to $F = 3$, even though that sequence of events is suppressed by a factor of 10^4. Therefore to combat the loss of atoms in the cooling process a repumper laser is kept on resonance from $F = 3$ to $F = 4$ to bring the atoms back into the process. Looking along any of the cardinal directions defined by the beams the atoms feel a force due to the optical molasses proportional to their velocity, v, in that direction, as can be seen in Equation (2.6).

$$\begin{aligned} F_{Doppler} &= \frac{\Gamma_{\text{res}}\hbar k}{1+(\frac{\Delta+kv}{\frac{\Gamma}{2}})^2} - \frac{\Gamma_{\text{res}}\hbar k}{1+(\frac{\Delta-kv}{\frac{\Gamma}{2}})^2} \\ F_{Doppler} &\approx -\frac{16k\Gamma^2\Delta\hbar k\Gamma_{\text{res}}}{(\Gamma^2+4\Delta^2)^2}v \end{aligned} \tag{2.6}$$

This approximation of the Doppler Force leading to a damping term proportional to velocity allows us to even examine what the optimal detuning is, where we define the optimal detuning to maximize the change in the force seen near zero velocity. For $\Gamma_{\text{res}} = \frac{\Omega^2}{\Gamma}$, the optimal detuning, Δ, remarkably enough, turns out to be $\frac{\Gamma}{2}$. While a cursory examination of the optical molasses might seem to imply that one could cool their sample down to the recoil limit for cesium, an extremely chilly 595.02 nK [41]. Upon closer examination one sees that as the velocity of the atom decreases its ability to preferentially scatter one helicity of light as opposed to the other decreases and the equilibrium temperature raises considerably to an energy on the order of $\hbar\Gamma$, or on the order of 100 μK.

While we have greatly confined the atoms in momentum space from where they started, we have yet to mention how a MOT is created that localizes the atoms

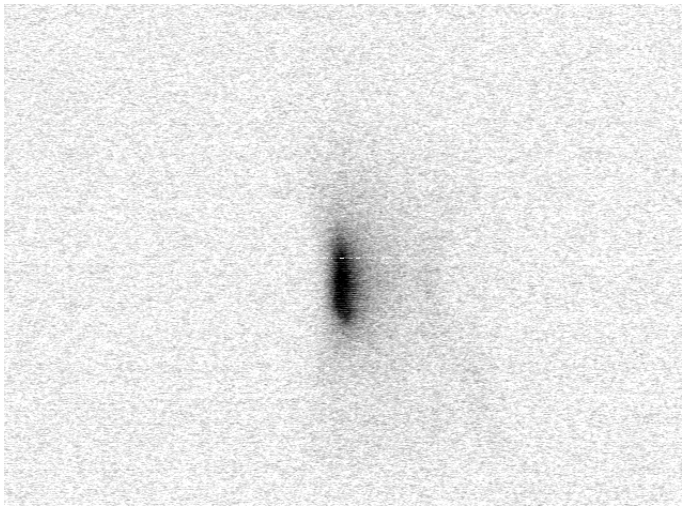

Figure 2-6: A sample of ultracold Cesium atoms localized in a MOT is visible without magnification when using an Infrared viewer. In preparing this figure, it was necessary to apply a nonlinear filter to this image taken with a CCD camera, but only for the means of visibility on paper.

spatially. By using Anti-Helmholtz coils inside our chamber we can create a linear magnetic field gradient inside. This magnetic field will split the magnetic sublevels with the distance between them increasing as atoms move farther from the center of the coils. Again, relying on preferential scattering arguments as detunings from resonance decrease as the energy of states change because of the B field, if we orient the B field correctly with respect to which direction σ^+ light propagates we can engineer it such that atoms will scatter more from counterpropogating beams as they leave the center of the coils [34]. In the whole, this effect is actually quite small until you consider the effects that preferentially scattering one helicity of light has on the state that the atom is in. The atoms by trying to leave the center of the coils are in fact optically pumped to the $F = 4$ stretched state (state of maximal angular momentum along the direction of quantization). In the stretched state more so than in any other state the atoms scatter even more of the counterpropagating light as the Clebsch-Gordan in that direction is much stronger. This further enhances the confinement to usable levels, allowing us to create a MOT small enough to be useful in addressing a significant proportion of atoms with our *Write* and *Read* beams while still being large enough to be seen by the naked eye, as in the photograph in Figure

2-6.

2.2.2 Polarization Gradient Cooling

The technique of introducing some preferential scattering into your system is widely used in all laser cooling experiments from creating a MOT to Sisyphus Cooling, Cavity Cooling [45], and Polarization Gradient Cooling (PGC). Compared to Doppler cooling, PGC cooling allows us to get much closer to the recoil limit as it does not rely solely on scattering induced by detuning. While a MOT requires there to be a magnetic field near the atoms PGC requires the field to be as close to zero as possible as all interactions and transitions are induced by the atoms being acted upon by the laser field.

By superimposing two counterpropagating circularly polarized beams with opposite helicity and same field amplitude an interesting shape is formed. In general, for the different field amplitudes, the component of the electric field moving in the positive direction is in Equation (2.7).

$$E^{+}(z) = \frac{1}{\sqrt{2}}\left(E_0' - E_0\right)\epsilon_x - \frac{i}{\sqrt{2}}\left(E_0' + E_0\right)\epsilon_y \tag{2.7}$$

Taking the field amplitudes to be the same we see that this complicated expression simplifies to a linear polarization. Expanding both the left moving and right moving part of the wave now, a simple relation between the polarization of this system and the distance along the direction of propagation can be derived, see Equation (2.8).

$$\begin{pmatrix} \epsilon_X \\ \epsilon_Y \end{pmatrix} = R_z(-kz) \begin{pmatrix} \epsilon_x \\ \epsilon_y \end{pmatrix} \tag{2.8}$$

This says that to find the basis where the polarization stays constant all that needs to be done is to perform a rotation of our fixed coordinate polarizations. Thus the polarization of the beam is constant in any one place, but is in the shape of a helix as it winds around down the direction of the propagation of the laser beam.

Going into a slowly moving frame similar to what an atom would see, and working

through the first order perturbation to the wave function we can see that there is coupling between the states that angular momentum were previously quantized in and states in other directions. Retaking the expected value of some angular momentum component operators, a non-isotropic distribution of angular momentum is discovered such that there exists a "Motion Induced Atomic Orientation" [11]. Similar to the way Zeeman shifts in a MOT cause preferential scattering of certain helicities of light, this motion induced atomic orientation makes it more likely for atoms to scatter photons from the beam that counterpropagates their motion such that kinetic energy from the atom is transferred to the scattered photon and the sample is cooled further. The difference of scattering events between counterpropagating and copropagating beams is on the order of $k\frac{\Gamma_{scat}}{\Delta}v$ where Γ_{scat} is the mean scattering rate of the cesium atom in its ground state and Δ is the light shift from atomic resonance. The force the atom feels is proportional to the number of scattering events times $\hbar k$. All that remains is to construct a coherent plan that includes both trapping atoms in a MOT and then cooling them with PGC.

To begin the sequence the MOT beams are turned on with the repumper set on the $3-4$ transition with the anti-helmholtz coils inside the chamber turned on and the bias magnetic field coils on the outside of the chamber turned on. After a short period of time the MOT coils are turned off, at which point the atoms are in the $F=4$ state with a temperature near 100 μK and are falling. After 2-3 ms the eddy currents in the vacuum chamber, caused by turning off the MOT coils, have rung down and the magnetic field near the atoms is zero thanks to the bias coils. The MOT beams are turned back on but this time they are tuned to depump the atoms from $F=4$ to $F=3$ as with no magnetic field the normally circularly polarized light looks unpolarized for each atom with its random orientation. To commence the PGC, the MOT beams turn off and the Repumper, which is circularly polarized, is shifted to the blue side of the $3-2$‘ transition by the computer controlling the sequence. We use the $3-2$‘ transition for PGC because of the large imbalance in Clebsch-Gordans due to the existence of a dark state. After 5 ms the atoms are at approximately 5 μK and are ready to be used for our experiment. There is nothing extremely

special about this sequence and there are many other plans one could think of for implementing both a MOT and PGC, but this is what gives us reliable results [31]. With our atoms cooled to very low temperatures we are now able to move forward with our experiment.

Chapter 3

Single Photon Generation Overview

The creation of a high-brightness source of single photons has long been a sought after prize in quantum optics [43]. The heralded single photon generating mechanism that we employ lends itself to a variety of applications ranging from quantum communication to probing the foundations of quantum mechanics, in studies of entanglement and metrology. In the following sections we will discuss the theory behind putting atoms in cavities, collective excitations, the technical details of how we implement our scheme for photon generation, and how by utilizing our source of single photons we can create a quantum memory for a single qubit.

3.1 Single Atoms vs. Collective Excitations

How does one create a single photon? Assuming we will collect the photon using a cavity, there seem to be two ways to create a photon: using a single atom or using N atoms. To understand why we have chosen to use multiple atoms we will examine the limitations imposed by using one atom to create single photons. As far back as 1946 Edward Purcell saw the great potential that placing atoms in cavities could have on the various emission processes [33]. To explain the enhancement of scattering into the cavity we will first look at this problem classically and then calculate it quantum

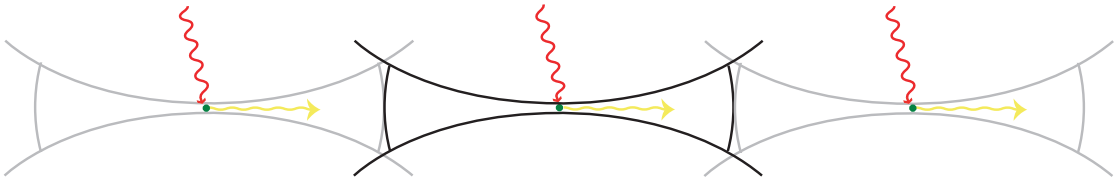

Figure 3-1: Atoms in the cavity witness enhancements in scattering rates into specific directions as if they were part of a phased array of atoms. This is caused by the imaging of the atom by the mirror a number of times equal to the finesse of the cavity.

mechanically. We define η to be the single atom cooperativity, a measure of the probability that a scattered photon will enter the cavity. Geometrically we know that η is nothing more than the solid angle subtended by the cavity mirrors over the total scattering area: $\frac{\Omega}{4\pi}$. On resonance the cross-section of an atom is equal to λ^2. Therefore the probability of scattering a photon from a beam of waste w is equal to $\frac{\lambda^2}{w^2}$. Upon first examination placing the atoms inside the cavity does not seem to offer any benefits, so how does the cavity enhance scattering?

Instead of imagining the cavity as a closed entity, picture each mirror surface as if it was a lens that just imaged the cavity and atom on the other side of the mirror. By utilizing the method of images and noting that the cavity is imaged a number of times equal to the average number of times a light pulse will bounce back and forth through the cavity, the Finesse, $\frac{\mathcal{F}}{\pi}$, one can see that all the image atoms will act as a phased array of emitters, Figure 3-1. By requiring constructive interference phased arrays greatly enhance emission along preferred directions in a narrow frequency range and are thus very useful in a wide variety of settings [26]. We can just as easily note that the light in the cavity will have $\frac{\mathcal{F}}{\pi}$ chances to scatter off the atom and therefore η will be enhanced by $\frac{\mathcal{F}}{\pi}$. Solving for the solid angle and using an approximation for the beam waist known as the 99 % criterion we find that η obeys Equation (3.1) [38].

$$\eta = \frac{3}{2\pi^3}\mathcal{F}\left(\frac{\lambda}{w_0}\right)^2 \tag{3.1}$$

Taking the results of Equation (3.1) one step farther we can ask what percentage of the photons scattered by this single atom in a cavity system will go into the cavity

mode compared to free space, the recovery.

$$\text{Recovery} \approx \frac{\eta}{1+\eta} \tag{3.2}$$

Before we move on, it is important to note that we did not have to use a classical argument to derive the single atom-cooperativity and the recovery. We could just have easily looked at this problem using quantum mechanics. The reformulation of this problem is simple: an excited state representing the atom in an excited state with no photons in the cavity with a linewidth equal to Γ is coupled by a constant g to a state with the atom in the ground state with one photon in the cavity mode with a lifetime κ as can be seen in Figure 3-2. As the rate at which the an atom Rabi flops from $|e,0\rangle$ to $|g,1\rangle$ is proportional to g^2, we know that to a reasonable approximation the rate a photon will be released into a cavity mode will be $\frac{g^2}{\kappa}$[1]. While the probability of seeing this decay will go like Equation (3.3) as any decays into free space are lost [9].

$$\frac{\frac{g^2}{\kappa}}{\Gamma + \frac{g^2}{\kappa}} \tag{3.3}$$

Which when we replace the quantities g, κ, and Γ with their equivalent expression in terms of classical quanties shows that $\frac{g^2}{\kappa\Gamma} = \eta$ gives us our normal equation for the expected recovery, Equation (3.2).

This is all well and good and is the basis for many other single photon experiments [19], however there are many technical challenges that make this technique less than perfect. First, the fabrication of a high-finesse small cavity to trap the atom in. Second, keeping the atom localized to less than an optical wavelength so as not to deconstructively interfere with the cavity scattering. Collective excitations offer a way around these challenges. Placing N atoms inside a medium finesse cavity one would assume that it would be impossible to easily scatter a single photon into the cavity mode, instead assuming that shining a laser onto the N atoms would lead to a poissonian distribution of N photons scattered into and out of the cavity. While this is true in the general sense, following a heralding scheme and selecting on specific

[1]This follows from Fermi's Golden Rule.

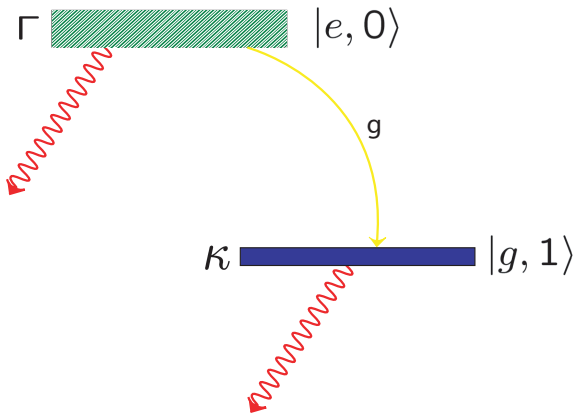

Figure 3-2: A two level system with linewidths equal to Γ and κ and a coupling of g between the levels. The higher level represents an excited atomic state with no photons in the cavity mode, while the lower level represents an atomic ground state with one photon in the cavity mode.

triggers that we will discuss shortly, one can use all the atoms as if they were a phased array of emitters with a greatly enhanced rate of scattering into the cavity mode, where the enhancement is $N\eta$. To fully understand this quantum phenomenon a small amount of formalism in notation must be introduced, but once this is done the reader will be delighted to see that nothing magical or out of the ordinary is taking place.

3.2 Fock State

The Dirac notation for quantum mechanics represented a great step forward in the understanding of modern quantum mechanics. Similar to the boon Feynmann diagrams gave to quantum field theory, the introduction of a notation that simplifies or at least obscures the mathematics of calculations is imperative to quickly forming a physical picture of one's system. At first glance however Dirac notation seems less than optimal to describe a system of N atoms or N photons. Furthermore a framework for discussing the electromagnetic field as a system of photons needs to be created. These rather embarrassing deficiencies are what the procedure known as Second Quantization is supposed to cure.

Taking a page from Classical Mechanics it is our intention to no longer treat the Schroedinger Wave Equation like a scalar, but rather treat it like a Classical Field Theory. We identify Canonical Coordinates, $\Psi(x,t)$ which is now an operator and its canonical partner Π, and perform the usual recipe for determining properties of these fields: writing an action consistent with the Lagrangian created by our field and setting the first order deviation of the action to be zero [8]. Following these prescriptions, $\Psi(x,t)$ is found to represent an infinite set of one dimensional harmonic oscillators. Each oscillator can be thought of as a different mode in the photon description of light, and each level of a each oscillator is another photon in that mode. Similar to the normal creation and annihilation operators there exist ${a_k}^\dagger$ and a_k whose commutation or anti-commutation relation is dependent on the class of particles the state is meant to represent. We will also define a Vacuum state by it's relation to these operators.

$$|\Omega\rangle \quad \Longrightarrow a_k |\Omega\rangle = 0 \quad \forall k \tag{3.4}$$

In general, these states are known as Fock States. The Hilbert space these states occupy, Equation (3.5), is a direct product space of smaller single particle Hilbert spaces which leads to the property that each component of these states individually obey the Schrodinger wave equation.

$$\mathcal{H} = h_1 \otimes h_2 \otimes h_3 \otimes \cdots \tag{3.5}$$

There however exists one unfortunate deterrence to the ordered beauty of this framework, namely the problem of ordering in the quantum mechanical operators that will act on the system. By blindly expanding all operators in terms of the creation and annihilation operators times the vacuum, and performing all the necessary commutators one discovers singularities. To combat this we normal order all of our operators before trying to take inner products between our states. The importance of this procedure will become clear in Section 3.5 when we are trying to count the number of photons we have created.

3.3 Write, Herald, Read

To generate a single photon from an ensemble of atoms we utilize a phenomenon known as Dicke Superradiance [13]. By creating a large symmetrized state over all the atoms addressed by our beams we are able to enhance certain decay processes to highly favor emission into the cavity. Without loss of generality we will analyze our procedure for an arbitrary 3 level system and then go into more specific models once the overall procedure is understood. Furthermore we will be using a pseudo Jaynes-Cumming Hamiltonian to quickly calculate the interactions between levels.

$$H_{JC} = g\left(a^{\dagger}\sigma^{-} \; + \; a\sigma^{+}\right) \tag{3.6}$$

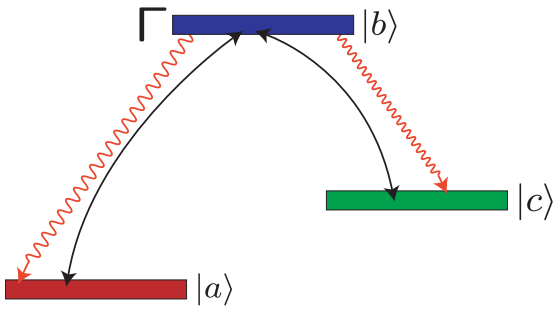

Figure 3-3: A three level system with a coupling between the two highest levels due to spontaneous emission as well as an external field.

Our hamiltonian will be similar to the one above as it is just describing a system in which absorption of a photon (a) leads to excitation of the atom, while emission of a photon ($a^{\dagger}$) leads to the lowering of the atom's energy state. In this treatment we will consider the action of our protocol on a system where the atom has three states available to it $|a\rangle$, $|b\rangle$, $|c\rangle$ seen in Figure 3-3.

Our intention in the following exercise is to create a closed 3 level system in which each state is a collective, well-symmetrized state of all the Cesium atoms. First, the sample of atoms is optically pumped such that all of the atoms are in the state $|a\rangle$ with zero photons in the cavity mode. We will label this state as the ground state of our system, $|G\rangle$, defined in Equation 3.7.

$$|G\rangle = |aaa\ldots aaa\rangle \otimes |0_{\text{cav}}\rangle \tag{3.7}$$

A weak coherent beam known as the *Write* beam is sent into the sample which is tuned to drive a single atom from $|a\rangle$ to $|b\rangle$. As discussed previously, we model this with a modified Jaynes-Cumming hamiltonian found in Equation (3.8).

$$H_{\text{Write}} = \Omega \sum_{j=1}^{N} |b_j\rangle \langle a_j| \, e^{i\vec{k_w}\cdot\vec{x}_j} + |a_j\rangle \langle b_j| \, e^{-i\vec{k_w}\cdot\vec{x}_j} \tag{3.8}$$

Here the j index refers not to separate components of a vector, but rather a different atom. One reaction was omitted from this hamiltonian as a photon is being either added to or subtracted from the *Write* beam itself, however this turns out to be inconsequential as we can easily model a laser as a coherent state, which is not effected by the removal of one photon.

Given our initial state $|G\rangle$ we act on it with the hamiltonian of the system defined by the action of the *Write* beam. The state we get out is a shared single excitation in which we know that one of the atoms has been excited to $|b\rangle$ but cannot tell which one. Therefore the state is a superposition of each atom having been the atom that was excited.

$$\begin{aligned} H_{\text{Write}} |G\rangle &= \left(\Omega \sum_{j=1}^{N} |b_j\rangle \langle a_j| \, e^{i\vec{k_w}\cdot\vec{x}_j} + |a_j\rangle \langle b_j| \, e^{-i\vec{k_w}\cdot\vec{x}_j} \right) |aaa\ldots aaa\rangle \otimes |0_{\text{cav}}\rangle \\ &= \left(e^{i\vec{k_w}\cdot\vec{x}_1} |baa\ldots aaa\rangle + e^{i\vec{k_w}\cdot\vec{x}_2} |aba\ldots aaa\rangle + \ldots \right) \otimes |0_{\text{cav}}\rangle \\ &= \Omega \sum_{j=1}^{N} e^{i\vec{k_w}\cdot\vec{x}_j} |b_j\rangle \otimes |0_{\text{cav}}\rangle \end{aligned} \tag{3.9}$$

The last line of Equation (3.9) is shorthand notation that we will continue to use throughout this discussion as we will assume that all atoms where the state is not specified are in the state $|a\rangle$. Taking the inner product of this new state with a normalized version defined in the Equation below,

$$|E\rangle \equiv \frac{1}{\sqrt{N}} \sum_{j=1}^{N} e^{i\vec{k_w}\cdot\vec{x}_j} |b_j\rangle \otimes |0_{\text{cav}}\rangle \tag{3.10}$$

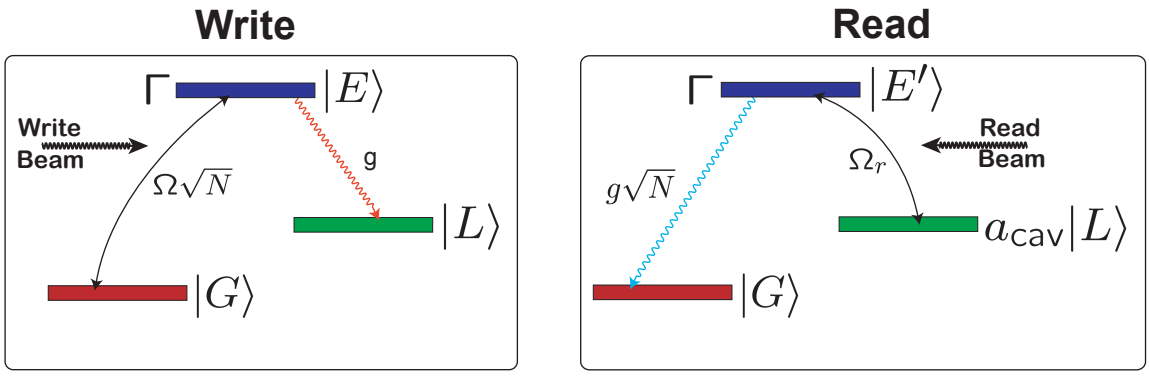

Figure 3-4: Two three level systems showing the sequence of events in both the *Write* and *Read* processes along with the relevant couplings between all the levels.

we can see what the coupling is between the two levels $|G\rangle$ and $|E\rangle$.

$$\begin{aligned}\langle E|\, H_{\mathrm{Write}}\, |G\rangle &= \sum_{i=1}^{N} \langle b_i| \frac{1}{\sqrt{N}} \Omega \sum_{j=1}^{N} |b_j\rangle \\ &= \sum_{i,j=1}^{N} \frac{\Omega}{\sqrt{N}} \langle b_i|b_j\rangle \\ &= \sum_{i,j=1}^{N} \frac{\Omega}{\sqrt{N}} \delta_{ij} \\ &= \sqrt{N}\Omega\end{aligned} \tag{3.11}$$

Knowing the coupling constant for this transition we can begin filling in the details of our 3 level system in Figure 3-4. We call this process of transitioning our atoms from state $|G\rangle$ to $|E\rangle$ the Write Process. While it might seem that we have miraculously already driven a collectively enhanced process, looking for one scattering event with N possible scattering centers would of course be enhanced by N. What follows next is the creation of our heralding photon from the decay of an atom in its excited state $|b\rangle$ to $|c\rangle$ as characterized by its linewidth Γ.

This heralding photon will in turn be detected by us and tell us whether the write procedure succeeded. The operators a_{cav} and $a_{\mathrm{cav}}^{\dagger}$ refer to the annihilation or creation of photons in the cavity mode which will in turn leak out of the cavity due to its finite linewidth κ. Without the *Write* beam on, the state is acted upon by an

operator C, referred to here on out as the cavity operator, defined in Equation (3.12).

$$C \equiv \sum_{j=1}^{N} g \left(\cos\left(\vec{k_c} \cdot \vec{x_j}\right) a_{\text{cav}} \left|b_j\right\rangle \left\langle c_j\right| + \cos\left(\vec{k_c} \cdot \vec{x_j}\right) a_{\text{cav}}^{\dagger} \left|c_j\right\rangle \left\langle b_j\right| \right) \tag{3.12}$$

We can now examine the coupling between state $|E\rangle$ and state $|L\rangle$ where the latter state is defined as the cavity operator acting on the former state properly normalized. For reasons that will become obvious later, this release of a photon into the cavity mode can be thought of as a successful loading of what some might refer to as a photon trap.

$$\begin{aligned} C\left|E\right\rangle =& g \sum_{i=1}^{N} \cos\left(\vec{k_c} \cdot \vec{x_i}\right) a_{\text{cav}}^{\dagger} \left|c_i\right\rangle \left\langle b_i\right| \frac{1}{\sqrt{N}} \sum_{j=1}^{N} e^{i\vec{k_w} \cdot \vec{x}_j} \left|b_j\right\rangle \otimes \left|0_{\text{cav}}\right\rangle \\ =& \frac{g}{\sqrt{N}} \sum_{j=1}^{N} \cos\left(\vec{k_c} \cdot \vec{x_j}\right) e^{i\vec{k_w} \cdot \vec{x}_j} \left|c_j\right\rangle \otimes \left|1_{\text{cav}}\right\rangle \end{aligned} \tag{3.13}$$

$$\left|L\right\rangle \equiv \frac{1}{\sqrt{N \sum_{l=1}^{N} \cos^2\left(\vec{k_c} \cdot \vec{x_l}\right)}} \sum_{j=1}^{N} \cos\left(\vec{k_c} \cdot \vec{x_j}\right) e^{i\vec{k_w} \cdot \vec{x}_j} \left|c_j\right\rangle \otimes \left|1_{\text{cav}}\right\rangle \tag{3.14}$$

In a less esoteric sense, if the heralding photon goes into the cavity mode what results is a phase grating that will later enhance the scattering of future photons into the cavity mode. Looking at Equation (3.14) we can see the appearance of this phase grating caused by the phase added to each term by the *Write* beam. All that remains is to see what the coupling is.

$$\begin{aligned} \left\langle L\right| C \left|E\right\rangle =& \frac{g}{\sqrt{N \sum_{l=1}^{N} \cos^2\left(\vec{k_c} \cdot \vec{x_l}\right)}} \sum_{j=1}^{N} \left\langle c_j\right| \cos\left(\vec{k_c} \cdot \vec{x_j}\right) \\ & \cdot e^{i\vec{k_w} \cdot \vec{x}_j} \frac{g}{\sqrt{N}} \sum_{k=1}^{N} \cos\left(\vec{k_c} \cdot \vec{x_k}\right) e^{i\vec{k_w} \cdot \vec{x}_j} \left|c_k\right\rangle \\ =& \frac{g}{N} \sum_{j,k=1}^{N} \delta_{jk} \\ =& g \end{aligned} \tag{3.15}$$

The heralding photon will help us post-select out only the trials that succeeded in creating this phase grating. We should note that this critical step in creating our phase grating is only enhanced by the cavity coupling constant, so in our case most of our photons never go into the cavity and create our collective state that we are looking for. So what do we do know that we have a phase grating?

While the phase grating itself is interesting and will be the fundamental building block of our quantum memory we will continue our exploration into how to retrieve a single photon from this system. The first step is to send in the *Read* beam. It should be noted that we are directing this beam in after the photon in cavity mode in state $|L\rangle$ has leaked out, therefore our initial state is now $a_{\text{cav}}|L\rangle$. Similar to Equation (3.8) the operator defined by the action of the *Read* beam is below.

$$H_{\text{Read}} = \Omega_r \sum_{j=1}^{N} |b_j\rangle\langle c_j| e^{i\vec{k_r}\cdot\vec{x}_j} + |c_j\rangle\langle b_j| e^{-i\vec{k_r}\cdot\vec{x}_j} \tag{3.16}$$

Once again we will look at the coupling between our initial state and a well-normalized version of what is generated by H_{Read} acting on our initial state.

$$\begin{aligned} H_{\text{Read}} a_{\text{cav}}|L\rangle =& \frac{\Omega_r \sum_{k=1}^{N} |b_k\rangle\langle c_k| e^{i\vec{k_r}\cdot\vec{x}_k}}{\sqrt{N\sum_{l=1}^{N}\cos^2\left(\vec{k_c}\cdot\vec{x_l}\right)}} \sum_{j=1}^{N} \cos\left(\vec{k_c}\cdot\vec{x_j}\right) e^{i\vec{k_w}\cdot\vec{x}_j} |c_j\rangle \otimes |0_{\text{cav}}\rangle \\ =& \frac{\Omega_r}{\sqrt{N\sum_{l=1}^{N}\cos^2\left(\vec{k_c}\cdot\vec{x_l}\right)}} \sum_{j=1}^{N} \cos\left(\vec{k_c}\cdot\vec{x_j}\right) e^{i\left(\vec{k_w}+\vec{k_r}\right)\cdot\vec{x}_j} |b_j\rangle \otimes |0_{\text{cav}}\rangle \end{aligned} \tag{3.17}$$

The normalized state, $|E'\rangle$, is equal to Equation (3.17) save for the omission of the Ω_r factor. Similar to the calculation of the *Write* decay process (3.15) taking $\langle E'| H_{\text{Read}} a_{\text{cav}}|L\rangle$ just gives us back this same coupling factor Ω_r. One last transition remains to be calculated to complete our sequence in Figure 3-4.

The transition between $|E'\rangle$ and the state which we are after $a^{\dagger}_{\text{cav}}|G\rangle$ where we

have created a heralded single photon is mediated by another cavity decay.

$$C' \equiv \sum_{j=1}^{N} g' \left(\cos\left(\vec{k_c} \cdot \vec{x_j}\right) a_{\text{cav}} \left|b_j\right\rangle \left\langle a_j\right| + \cos\left(\vec{k_c} \cdot \vec{x_j}\right) a_{\text{cav}}^{\dagger} \left|a_j\right\rangle \left\langle b_j\right| \right) \tag{3.18}$$

The difference between cavity coupling constants g and g' are merely multiplicative factors whose roots come from the different Clebsch-Gordan coefficients from decaying into different levels.

$$\left\langle G\right| a_{\text{cav}} C' \left|E'\right\rangle = \frac{g'}{\sqrt{N}} \sum_{j=1}^{N} e^{i\left(\vec{k_w}+\vec{k_r}\right)\cdot\vec{x}_j} \tag{3.19}$$

$$= g'\sqrt{N} \tag{3.20}$$

It is this final process that exhibits the collective enhancement we have been seeking this entire time. Furthermore the recovery we discussed earlier comes directly from this process which has a rate of Ng'^2 which when combined with the decay channels in the cavity and atom lead to our normal recovery of $\frac{N\eta}{1+N\eta}$.

3.4 Implementation Details

Throughout this chapter the discussion has been kept on a highly abstract level. To bring this topic more down to earth we will, in this section, focus on some of the more technical details of implementing this single photon generation procedure and subsequently the quantum memory or buffer. For purely practicable reasons all of our experiment is centered around the D_2 line of Cesium. As indicated in Figure 3-5 to the right, by utilizing the hyperfine structure of Cesium there are a plethora of easily accessible levels that can be used for optical pumping and our experiment. Given the small frequency spacing between the $\left|6P_{\frac{3}{2}}\right\rangle$ hyperfine states we can easily use EOMs in conjunction with AOMs to quickly change which transitions we are addressing mid-sequence. There is an even greater degree of freedom afforded to us by the use of a cavity, the degeneracy created between frequencies an integral number of Free Spectral Ranges apart.

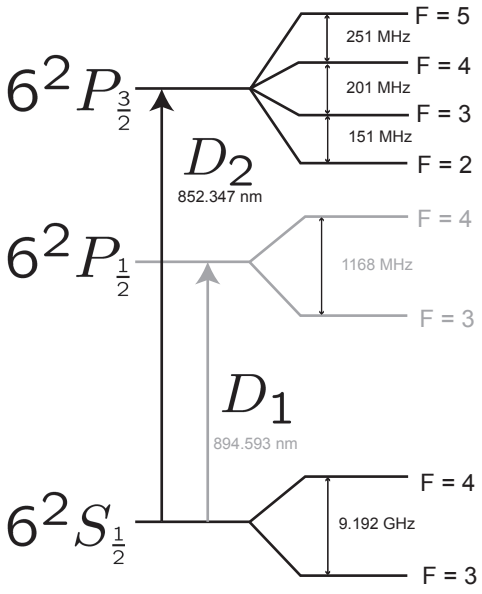

Figure 3-5: An energy level diagram showing the separation of the Hyperfine energy levels in the Cesium atom. All splittings were obtained from Reference [41].

3.4.1 Pound-Drever-Hall Cavity Lock

In considering a standing wave present in an optical cavity, one should notice that the only condition for constructive interference inside the cavity is that the phase of the wave needs to change by an integer number times 2π. As such there exist an infinite set of frequencies of light that will fit inside this cavity as long as they satisfy the condition that $2\pi\nu\frac{2L}{c} = d2\pi$ where d is an integer. The distance between each of these frequencies is known as the Free Spectral Range and is an innate feature of any optical cavity.

$$\Delta\nu_{\text{FSR}} = \frac{c}{2L} \tag{3.21}$$

Therefore any beams we use to interrogate the atoms can be scattered into the cavity as long as their frequency is an integral number of FSRs. The standing wave cavity that we use has a measured FSR of 2.266 GHz. In the past, this has allowed us to use different lasers for our read and write beam at different frequencies that differed by 4 FSRs from each other.

An important fact to take away from this is how important cavity length is to

constructive interference. While earlier we argued that scattering light from atoms into the cavity was enhanced by the finesse, it was explicitly assumed that the atoms were stationary to within an optical wavelength, most importantly however it was implicitly assumed that the cavity did not change its length. As variation in the length of the cavity will destroy the cavity induced enhancement just as easily as movement of the atoms would. To accomplish this cavity length stabilization we will employ a Pound-Drever-Hall lock with a frequency stabilized laser and vary the length of the cavity, not the laser frequency [5].

Mounting one of the cavity mirrors on a piezoelectric ceramic crystal allows us to change the length of the cavity, however a lot more precision is needed than just gross length corrections. The cavity can be treated just like a normal Fabry-Perot resonator which only transmits light at or near multiples of the free spectral range. When the cavity is the correct length to transmit the light of our locked cavity laser there will be little to no reflection from the input mirror. It should be noted that this signal is not just a first order reflection of the input beam but also the light that leaks out of the cavity through the input mirror. On resonance these two will be totally out of phase and will destructively interfere to null this signal. Unfortunately there exist many problems for using this nulling intensity signal for the cavity lock. First, the signal is symmetric about zero and it would be difficult to discern which direction a cavity length change should be in. Second, any amplitude noise on the cavity laser would look like a change in the signal we are trying to stabilize. The solution is quite simple in fact, instead of looking at intensity, we look at the derivative of intensity which is antisymmetric about the resonance.

To get a DC voltage that can be used as an error signal for the piezo driver we will add phase modulation to the cavity laser. By introducing a phase modulation at a frequency Ω the original beam, with frequency ω_{cav}, now acts as a carrier with two sidebands at frequencies $\omega_{\text{cav}} \pm \Omega$. By performing the exact calculation of the intensity of the reflected beam it turns out the phase information we are looking for is on a term coupled to $\sin(\Omega t)$. To retrieve this signal we pick off the reflected beam and measure its intensity with a fast photodiode. We then demodulate the signal

with a frequency Ω and the original modulation signal, which must be fed through a manually tuned delay line so as to be in phase with the light. Finally we pass our signal through a low-pass filter, to get rid of all the high frequency noise, and we are left with a DC error signal that can be fed into a normal control loop for the piezo drivers. With the cavity length stabilized we are able to enhance the scattering of light into the cavity.

All that remains to creating a heralded source of single photons is the ability to detect single photons. For our purposes we are able to use commercially bought Single Photon Counting Modules (SPCMs) from Perkin-Elmers. At the wavelength we currently are working at these detectors have a Quantum Efficiency (QE) of 40%. Finally with all this explained we are ready to create single photons and it is now only a matter of proving that we have succeeded.

3.5 g_2 Measurement

While we can perform our heralding photon generation scheme and see that it works, we have yet to discuss how the photons we get from this procedure are any different from attenuated laser light. One of the other popular choices for creating single photons is thematically similar to just placing attenuators in a laser's path until only a few photons can pass through all the attenuators. These light sources act in a classical manner following poissonian statistics. Therefore the probability of getting n photons in such a process is equal to the probability of having n events coincide according to a poisson distribution. For our purposes, as events with three or more photons are greatly suppressed, all we are interested in is the probability of getting two photons, P_2, which classically is quite simple.

$$P_2 = \frac{1}{2}{P_1}^2 \tag{3.22}$$

Our single photon source should break the equality in Equation (3.22), by suppressing the probability of multi-photon creation.

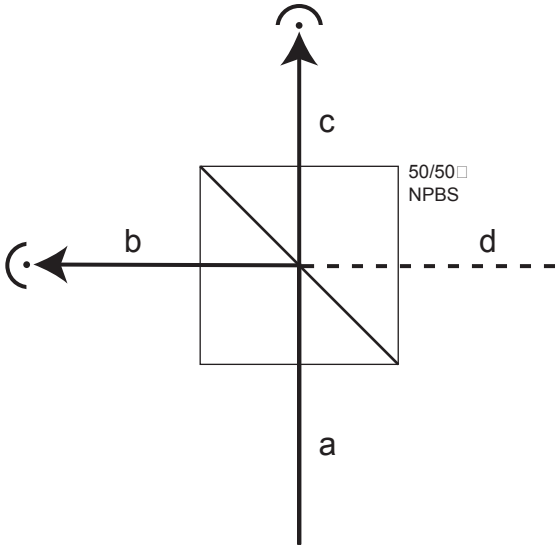

Figure 3-6: A Hanbury-Brown Twiss interferometer with all 4 ports labeled, including a vacuum port.

Two quantities will play an important role in our discussion of photon statistics: $\langle n_w \rangle$ and $\langle n_r \rangle$ the average write rate and the average read rate. The write rate is a measure of how often a heralding photon is emitted into the cavity mode. As one should remember the scattering of a photon into the cavity mode on this leg of the scheme was not collectively enhanced and this quantity will be quite small. Write rates for recent experiments have been on the order of a few percent, most recently 2%. Read rates are a measure of how often the final photon is observed. Thankfully due to our high recovery caused by collective enhancement back, the read rate is on the order of the write rate. Both of these measures are very useful for immediate evaluation of new data when an experiment is being performed.

The ultimate measure of whether our photons show signs of sub-poissonian statistics is the g_2 or $g_{\mathrm{rr—w}}$ measurement, the read auto-correlation given a write photon

[37].

$$g_2 = \frac{\langle : n^2 : \rangle}{\langle n \rangle^2} \tag{3.23}$$

$$= \frac{\langle : a^\dagger a a^\dagger a : \rangle}{\langle a^\dagger a \rangle^2} \tag{3.24}$$

$$= \frac{\langle a^\dagger a^\dagger a a \rangle}{\langle a^\dagger a \rangle^2} \tag{3.25}$$

$$= \frac{\langle n^2 - n \rangle}{\langle n \rangle^2} \tag{3.26}$$

Classically this normalized auto-correlation will always be greater than or equal to 1 [28]. Measuring these photon statistics on a Hanbury Brown-Twiss interferometer like Figure 3-6 one finds that regardless of the interferometry method one uses to get to the final answer the g_2 does not change and the autocorrelation of the total number of photons is equal to the cross correlation down paths b and c of the interferometer. The g_2 also has one more interpretation that can be quite useful.

$$g_2 = \frac{P_2}{\frac{1}{2} P_1^{\,2}} \qquad \text{Classically} \tag{3.27}$$

With this expression the non classical requirement that g_2 must be less than 1 is much more obvious. For the this experiment three SPCMs were utilized to analyze the g_2 of our generated photons, 1 SPCM to catch the heralding photon, and the other two to create a Hanbury Brown-Twiss interferometer. This measurement is especially time consuming as we must wait until multiple 3-photon events are observed to get a good limit on our measured value for g_2 which was 0.24(6). This takes a considerable amount of time as not only must this even occur, but also we need to successfully measure all three photons, a process that is suppressed by the detection path quantum efficiency to the third QE^3, $\frac{1}{1000}$ in this experiment.

A less reliable but more useful measure in a day-to-day lab setting is the intensity cross-correlation g_{wr}.

$$g_{\mathrm{wr}} = \frac{\langle : I_w I_r : \rangle}{\langle I_w \rangle \langle I_r \rangle} \tag{3.28}$$

A modified Cauchy-Schwarz inequality signals that classically the field cannot have a higher cross correlation than auto-correlation for each of the two photons.

$$\frac{{g_{\mathrm{wr}}}^2}{g_{\mathrm{ww}}g_{\mathrm{rr}}} \leq 1 \qquad \text{Classically} \tag{3.29}$$

Unfortunately, as was mentioned before, the measurement of g_{rr} takes a long time and requires 2 detectors (the same can be said of g_{ww}) as such it is not an extremely practical inequality to check during each experimental run. Most of these quantities can be described at a specific time, but for our purposes we will only talk about the various correlation values at time $t = 0$. In our experiment $g_{\mathrm{wr}} \approx 6$ and $g_{\mathrm{rr}} = g_{\mathrm{ww}} \approx 2$. This of course leads to a strong violation of the Cauchy-Schwarz inequality.

Looking at the expression for g_{wr} in Equation (3.28) we can rewrite this using experimental quantities.

$$\begin{aligned}
g_{\mathrm{wr}} =& \frac{\langle : n_w n_r : \rangle}{\langle n_w \rangle \langle n_r \rangle} && (3.30)\\
=& \frac{P(r\&w)}{P(r)P(w)} && (3.31)\\
=& \frac{P(w)P(r|w)}{P(r)P(w)} && (3.32)\\
=& \frac{n_w \chi q^2}{n_w \left(n_w \chi + B\right) q^2} && (3.33)\\
=& \frac{1}{n_w + \frac{B}{\chi}} && (3.34)
\end{aligned}$$

Here B is the probability of getting a background count in our detectors, χ is the recovery efficiency, and q is the quantum efficiency of our detectors, leaving us with a simple equation that tells us how the autocorrelation between rights and reads scale [25]. Given our write rate of .02 we see that at a minimum our g_{wr} should be 50, instead it is 6 telling us that we are strongly background limited and cannot easily increase our signal. Regardless these results tell us that we have created a high-efficiency source of heralded single photons and it is time to move on to how we create a storage device for quantum information.

3.6 Towards A Quantum Memory

In classical computation one uses a **bit** as the smallest unit of information. A bit can take on the values of 1 or 0 and is represented usually as high or low voltage. The digital abstraction was introduced in the design of modern electronics to allow one to make a record of the entire state of one's classical system. By disentangling the notion of a continuum of states an analog system could exist in and the amount of information an analog system could encode, we are able reproduce the state of a digitzed system exactly. Quantum information is different as there is no simple discretization process which when reproduced will approximate the behavior of your original quantum system exactly. Therefore we must define a new quantity that can encode all the information in a quantum system. A **qubit** is a single particle in a superposition state of a two state system, $|\psi\rangle = a|0\rangle + b|1\rangle$, where the states $|0\rangle$ and $|1\rangle$ are orthogonal. By modifying the protocol for single photon generation, the polarization state of a *Write* photon, Equation (3.35), will be shared between two magnons and released at a time of our choosing as if it was stored inside a some kind of quantum analog to a classical memory.

$$|\psi\rangle_{\text{photon}} = \cos(\theta)|+\rangle + e^{i\phi}\sin(\theta)|-\rangle \tag{3.35}$$

The first change to the original scheme will be to the polarization of the optical pumping. Instead of pumping with σ^+ or σ^- light on $3-4'$ which would put our sample of Cesium atoms into one of the stretched states with maximal (or minimal) angular momentum projection, we instead pump with π polarized light on $3-2'$. Successive bursts of optical pumping drive our sample of Cesium atoms into two groups: A, $|F=3, m_f=-3\rangle$, and B, $|F=3, m_f=3\rangle$. As can be seen in Figure 3-7, we can treat this as two Fock states which will obey the same principles that the single Fock state obeyed in our discussion of single photon generation earlier.

Assuming that we define the $\hat{z}$ direction to point along the cavity, our optical pumping beam will be polarized along the $\hat{x}$ direction and enter the chamber in the $\hat{y}$ direction as seen in Figure 1-1. Our *Write* beam tuned from $F=3$ to $2'$ is propagating

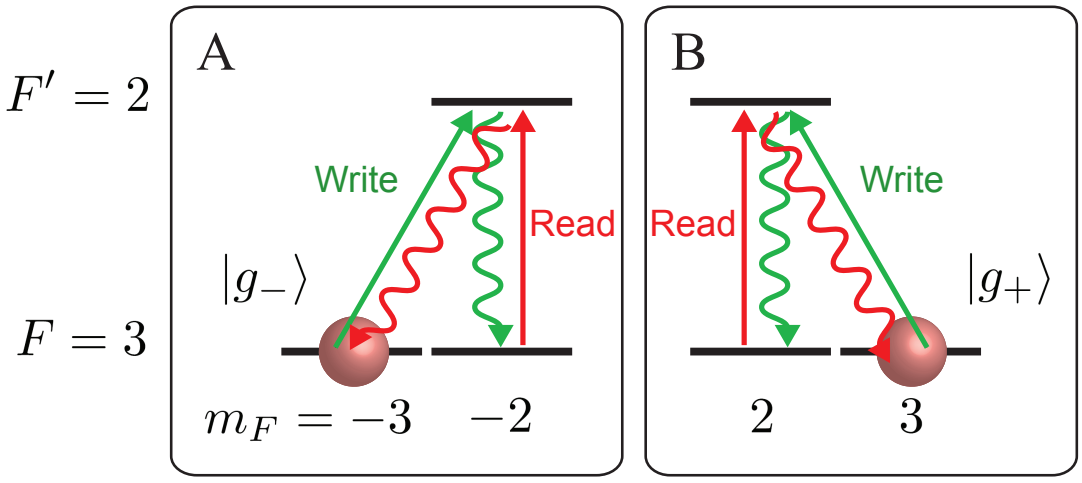

Figure 3-7: An illustration showing how both samples A and B will emit/absorb π polarized photons in a similar manner and how their neighboring hyperfine states are fashioned into a closed three level system. $|g_\pm\rangle$ indicates whether the state $|G\rangle$ corresponds to a set of atoms with maximal angular momentum projection or minimal [42].

along the $\hat{x}$ direction and therefore any photons initially scattered into the cavity that are π polarized will create entanglement between samples A and B. Note, we did not have to invoke which sample A or B scattered the photon to know that if it went into the cavity and was π polarized that each would respond in the same manner. This choice of polarization selection and propagation axes was specifically chosen such that the identity of the sample which scattered the photon would be obscured almost like a quantum eraser in a double-slit experiment. Intentionally obscuring this fact creates a state that is a direct mapping from the polarization state of the photon, Equation (3.35), to an entangled state of magnons A and B in Equation (3.36) thereby transferring all of the information contained in the polarization qubit [42].

$$|\psi\rangle_{Atomic} = \cos(\theta)\,|1\rangle_A\,|0\rangle_B + e^{i\phi}\sin(\theta)\,|0\rangle_A\,|1\rangle_B \tag{3.36}$$

What of the *Read* process, is that changed? We must again find a way to drive both the shared excitation in sample A and that in sample B back to their respective stretched states. A π polarized beam along the $\hat{x}$ direction would accomplish this but

it is here that problems start to arise. Looking back at the requirements for collective enhancement on the read process we are reminded that the *Read* and the *Write* beam must be counterpropagating. This of course poses a problem as the *Read* beam cannot be polarized along its direction of propagation. Therefore a rather unconventional solution was decided upon, instead of having a stationary static sample we would instead have its magnetic moment be rotating throughout the experiment. A B field of 1.4 Gauss in the $\hat{y}$ direction created by our Helmholtz coils induces Larmor precession with a period $\tau_L = 2\ \mu s$. Thereby allowing us to wait $\frac{1}{4}$ of a period after the *Write* and send in light polarized along the $\hat{z}$ which will look like the needed light along the atoms' now rotated quantization axis. In the time between our *Write* and *Read*, the polarization is stored between the two magnons so we will call this time the Quantum Memory storage time.

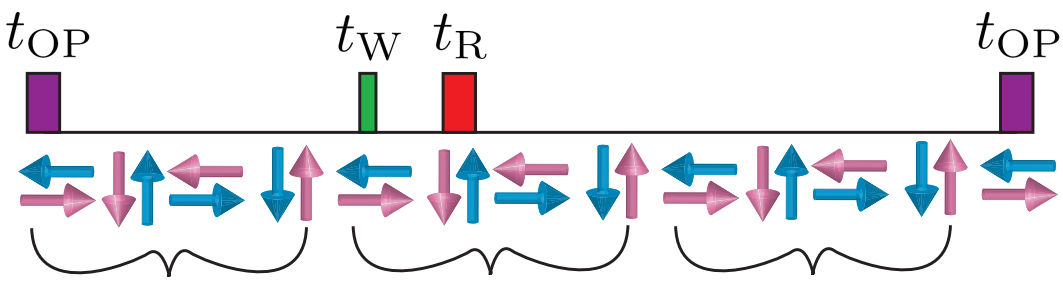

Figure 3-8: The pulse sequence situated above an illustration of where the collective atomic spin is pointing at each moment during the sequence [42].

An experimental sequence for this rotating scheme is quite simple, and can be easily visualized like in Figure 3-8. First the *Write* beam goes on for 50 ns at a low enough power that in each run we only excite n_w atoms. One quarter of a period later, the *Read* beam is turned on for 100 ns. Lastly, at 2 μs into the sequence the optical pumping is turned on for 75 ns. To prove that there is no overall optical pumping effect from having the same sample always be addressed as the $m_f = -3$ or $m_f = 3$ state, each trial is made 3 μs long so that every trial which magnon is the one with maximal angular momentum is switched. And finally 10,000 trials are performed between repetitions of the laser cooling sequence.

Results from this method of polarization storage are presented in Chapter 5 how-

ever it is a good time to reflect on what has been accomplished. Starting with atoms in a high vacuum chamber we have cooled and trapped them and have demonstrated exquisite control over their internal energy structure. Using techniques of atomic manipulation invented in the 1950s with computer controlled timing cards accurate to the nanosecond we are able to control quantum states shared across thousands of atoms, create a sub-poissionian source of single photons, and even store a single qubit.

Chapter 4

Implementation of Long-Lived Polarization State Storage

While a plan for the construction of a quantum memory was given in the previous chapter there are many challenges that must be overcome. First, the requirement that our sample be actively rotating throughout our experiment has transformed the routine procedure of optically pumping our sample of Cesium atoms into a much more dynamic problem. Second, the storage time of the quantum memory is only limited by the decoherence of our atoms' shared excitations. After a brief introduction to the general technique of optical pumping and a discussion of how we implemented optical pumping for our rotating sample, two decoherence mechanisms will be explained along with our attempts at minimizing their effects on the experiment with the installation of an Optical Lattice.

4.1 Optical Pumping

First demonstrated in 1949 by Kastler optical pumping is the process of polarizing a sample of atoms by creating a large population imbalance by means of inducing transitions in magnetic sublevels by flooding the atoms with light [17]. Application of the Wigner-Eckhart Theorem for electric dipole transitions provide selection rules that can be used to map the evolution of the system to its steady state as it absorbs

and emits photons. In many of the discussions earlier we assumed this led to a sliding of an entire atomic population to one of the stretched states, or more generally a dark state where the atom cannot scatter any photons due to the selection rules. To create our two samples that will be entangled by our storage photon, two atomic dark state populations emerge as we send in π polarized light. Over long times, the two polarizations of light send the populations to opposite ends of the magnetic sublevels of $F = 3$ as eventually through a random walk of scattering events the atoms decay into one of the two dark states. A steady state solution is reached when the optical pumping time,τ_{OP}, is much greater than the lifetime of the excited state: $\tau_{\mathrm{OP}} > \Gamma$. However, in a rotating sample, we are not afforded the luxury of optically pumping for as long as we want and the problem requires further analysis.

4.1.1 Optically Pumping a Rotating Sample

Trying to optically pump a sample of atoms in a homogeneous magnetic field introduces a number of issues that limit our ability to effectively polarize the sample. In constructing a MOT we saw that, on average, each time a photon Raman scatters off an atom, an impulse is felt by the photon. This impulse adds to the momentum and kinetic energy of the atom. This in turn heats up the atoms, increasing their predisposition to decohere our state and thereby limiting the amount of time we would like to send an optical pumping beam into the sample if the atoms are not safely inside a dark state. In contrast to the upper limit on pumping time, the finite linewidth of the excited state enforces a minimum amount of time needed to scatter one photon, $\frac{2}{\Gamma}$, which is approximately 60 ns. By more fully analyzing the effect the rotation has on the amount of heating, we can get a better idea of what the trade offs are of changing the length of the optical pumping pulse.

Classically one could describe Larmor Precession as the rotation of a magnetic moment around a magnetic field caused by the torque, $\tau = \vec{\mu} \times \vec{B}$. However this does not give us any insight into how atoms in the dark state start to scatter photons once the quantization axis has moved past where it was when the atoms were first polarized. As the atoms must cycle through the all the magnetic sublevels in a single

period we expect that some coupling between levels must be created. It is now worth recalling that our choice of this irreducible representation of our state in terms of the quantum numbers F_x and m_{f_x} was purely a matter of convenience and the state can be recast in another basis at any time. Thus once the sample has been rotated we could rediagonalize the states using a basis that itself has rotated with the atoms. Therefore the amount of coupling between any two states will just be equal to the inner product of the two states with a rotation acting on one of the states. One could most easily calculate the final product by decomposing the states into the basis of the rotation, in this case $\hat{y}$.

The first example of such a calculation can be found in Equation (4.1) [44].

$$\left|\langle f, f|e^{i\beta\sigma_y}|f, f\rangle\right|^2 = \cos^{2f}\left(\frac{\beta}{2}\right) \qquad \text{where } \beta = \omega_L t \tag{4.1}$$

Lo and behold, the answer is exactly what we would expect classically as the coupling of the level to itself turns out to be periodic with a frequency corresponding to the Larmor period. Performing this calculation for coupling to the nearest magnetic sublevel state, $f-1$, we can find an approximate answer for the coupling between the dark state and the adjacent state for small t.

$$\left|\langle f, f|e^{i\beta\sigma_y}|f, f-1\rangle\right|^2 = \frac{f}{2}\beta^2 + O\left(\beta^4\right) \tag{4.2}$$

So assuming that we center our optical pumping pulse of length τ_{OP} at the exact moment the polarization of the light and the quantization axis are the same we can to a good approximation calculate the heating caused by trying to optically pump while the sample is rotating. Equation (4.3) gives us a measure of the number of scattering events for one Larmor period per atom per trial.

$$\int_{-\frac{\tau_{\mathrm{OP}}}{2}}^{\frac{\tau_{\mathrm{OP}}}{2}} \Gamma_{\mathrm{sc}}\frac{f}{2}\beta^2 d\tau = \frac{f}{24}\omega_L^3\tau_{\mathrm{OP}}^3\Gamma_{\mathrm{sc}} \tag{4.3}$$

So by requiring that $\tau_{\mathrm{OP}}\Gamma_{\mathrm{sc}} \approx 1$ we see that backgrounds induced by the rotation are not small, and it is greatly in our interest to optimize our optical pumping. To

perform this optimization we will try to maximize both the number of atoms that are polarized and the accuracy with which we place the optical pumping window in the experimental sequence.

4.1.2 Probing Through the Cavity

By maximizing the number of atoms in the polarized sample we expect that by changing the frequencies of lasers, the alignment of the lasers onto the atoms, or the timing of pulses we intend to see a larger number of atoms involved in optical pumping. But how are we to measure the number of atoms? The answer lies in exploiting the cavity. Light sent through an empty cavity will show a transmission peak at the cavity resonance plus all the peaks separated by an integral number of FSRs away from resonance. However, a cavity with atoms in it will exhibit a very different transmission spectrum. Due to a phase shift induced by the photons of the probe beam hitting the atoms the transmission intensity versus the frequency of the probe beam will be a double peaked structure [46]. Denoted the Vacuum Rabi Splitting the peaks themselves will exhibit a width of $\frac{\kappa+\Gamma}{2}$ and will be separated by $g\sqrt{N}$ where N is the number of atoms that are polarized.

To see this signal we send in a weak circularly polarized beam through the cavity while constantly sweeping its frequency across the cavity resonance; we then monitor the transmission using a fast photodiode, one of which I constructed, and display it in real time on an oscilloscope. Figure 4-1 shows an example of what would normally be seen on the oscilloscope. As interpreting this signal is extremely easy, it serves as a fantastic diagnostic tool to use for optimizing optical pumping or seeing how other beams might heat the atoms. It is even routine to send in a superposition of two circular polarizations of light, lin polarized light, and divide the signal onto two photodiodes, one for each polarization. One could be used to probe a dark state population and the other could be used to probe states that we hope would be empty, allowing us to optimize our optical pumping by both maximizing one signal's separation and minimizing the other's. In the quantum memory experiment a weak π polarized beam along the $\hat{x}$ direction is sent through the cavity and picked up at the

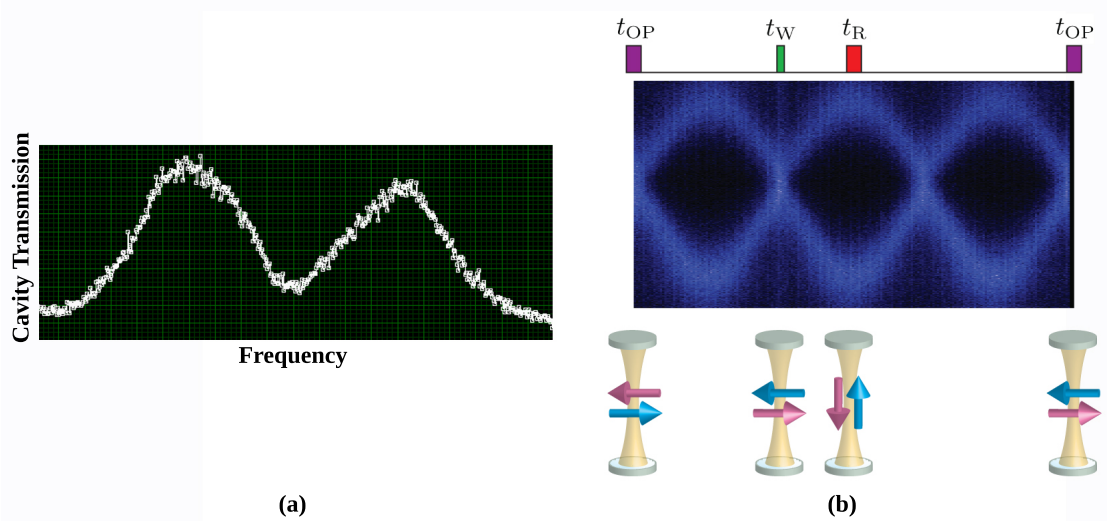

Figure 4-1: (a) A representative measurement of the vacuum Rabi splitting measured with a probe beam sent through the cavity. (b) A measurement of vacuum Rabi splitting as it changes in time due to the precession of the samples' magnetic moments. The timing of events in our sequence, and the orientation of the magnetic moments throughout the sequence is shown. The sequence is timed to coincide with the desirable orientation of the magnetic moments [42].

other end. Tuned to the $F = 3$ to $F = 2'$ transition, the stretched states as they were originally defined should not cause any splitting. However as the sample is rotating it is obvious that some splitting should reappear.

As we know that the Larmor precession of our sample expressed in couplings between magnetic sublevels is somewhat sinusoidal we expect the vacuum Rabi splitting observed to be similarly sinusoidal. Every time the sample is polarized in the $\pm\hat{x}$ direction we know that if we are correctly pumped then no splitting will occur. By symmetry arguments, at a quarter and three quarters of the Larmor period the greatest splitting will occur. So scanning the probe laser's frequency again and again and connecting all the line plots we can measure the Larmor precession, as can be seen in Figure 4-1. This provides us with a valuable tool to tweak the timing of all of our pulses to align with the atoms' orientation throughout the experimental sequence.

4.2 Signal Degradation

A whole host of effects cause a degradation in the recovery signal that is normally unaccounted for. These unexpected outcomes are caused by a range of antecedents from static emergent properties of the system to dynamic losses out of our system which can be described by Lindbladt operators or non-hermitian processes. Drawing examples from both of these extremes we will examine the variability of recovery due to the position of the MOT in the cavity and we will discuss the leading limit to our memory storage time: Doppler Decoherence.

4.2.1 Standing Wave in the Cavity

When considering the requirement for counterpropagation between the *Read* and the *Write* beams the ability to separate them by 4 FSRs seemed to be the ideal solution to making sure that both ground states of Cesium were driven to the same excited state. Lurking beneath our naive use of the free spectral range to get what we wanted was a dark detail that could potentially have destroyed the entire recovery signal. For a better understanding of how we might destroy our recovery we must recall exactly what the free spectral range tells us about our cavity.

The FSR tells us what the minimum spacing is between any two frequencies that would fit into our cavity. As we have chosen the two beams to be on resonance with the cavity we know our *Write* frequency fits into our cavity with its field following some kind of $\sin(k_w x)$ behavior such that it has a node at both mirrors. A frequency that is one FSR away from k_w will also have nodes at both ends of the mirror, but as it is the absolute minimum increase in frequency that still fits inside the cavity the two waves will start in phase, but the higher frequency field will be 180° out of phase with the lower frequency field at the second mirror. When calculating the recovery from a sample that spans a finite length of the cavity a spatial integral will have to be evaluated. The problem emerges from the point in the cavity where the two beams are 90° out of phase such that the spatial profile of the two beams when integrated over multiple optical wavelengths is similar to $\int_0^{\frac{2\pi}{k_w}} \sin(k_w x)\cos(k_w x)dx$ which obviously is

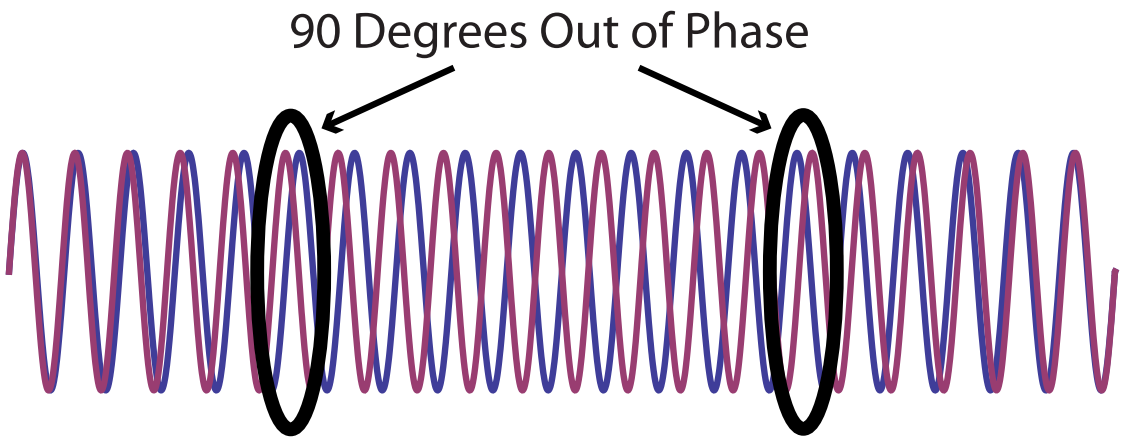

Figure 4-2: An example of how the phase between two modes, separated by 2 FSRs, changes inside the cavity. As an entire wavelength is "lost" between the two mirrors, there exist two points that are 90° out of phase with each other and will exhibit no recovery if the MOT is placed there.

equal to zero. Similarly, for beams separated by two FSRs there are two points in the cavity out of phase by 90° as can be easily seen in Figure 4-2.

In our present scheme with the *Read* and the *Write* separated by 4 FSRs there are four regions that would give us zero recovery. Near the center of our cavity the space between two regions of low recovery is only separated by 1.65 *cm*. Therefore it is extremely important to localize our MOT to a region of high recovery. To map the variability one could imagine moving the MOT, optical pumping lasers, and other lasers repeatedly and seeing the variation in the recovery due to MOT placement in the cavity. However, by itself, such an exercise would be tedious and would not be particularly informative as there are a large number of systematic changes in the signal that occur. A much simpler way of partially mapping this variability in recovery is at each point of mapping the recovery to change the frequency of the *Write* beam which changes the pattern of low recovery points. This experiment was done using a simple single photon generation scheme by writing in with the write separated from the read by 3 FSRs and by 4 FSRs and taking the ratio of these two recoveries, thereby cancelling out the systematic changes of moving all the beams around. The results can be found in Figure 4-3. When performing the quantum memory experiment the MOT was placed in a region of high recovery.

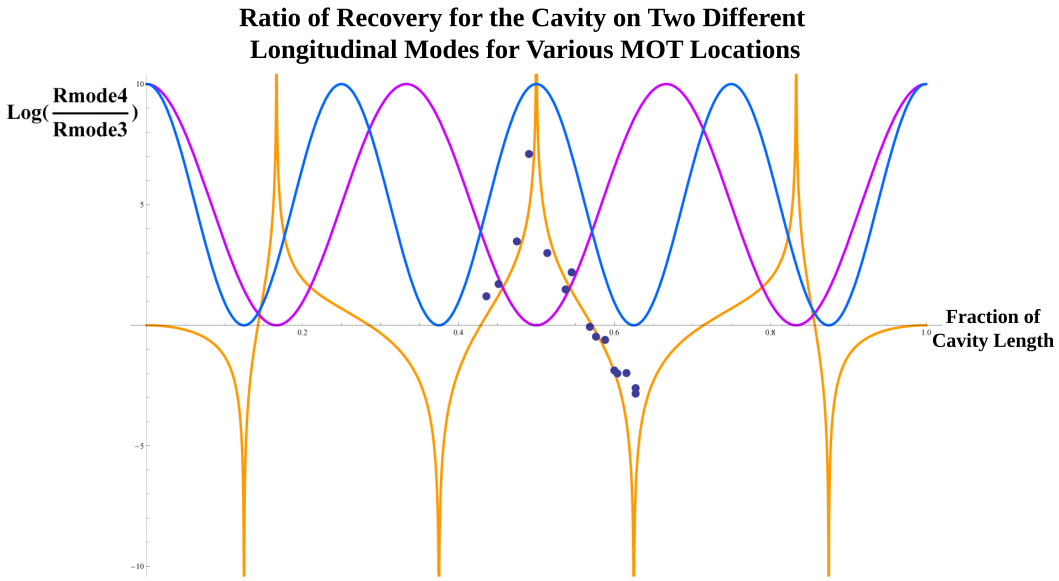

Figure 4-3: Plotted above is the Log of the expected recovery of two different detunings of the *Write* beam, separated by one free spectral range versus the MOT's position in the cavity. To cancel systematic changes in recovery from moving the MOT around, the data is plotted as the log of the ratio of these two recoveries. As one can see there is a high level of correspondence between the data and the theoretical model, the orange line.

4.2.2 Doppler Decoherence

Doppler decoherence is best described as the dynamic degradation of quantum coherence due to the thermal distribution of velocities in an atomic ensemble. In our early attempts to describe our system of particles during the *Write* and *Read* process we assumed that the velocity of our atoms was zero such that they did not move during or after the process. The collective excitation properties of our atomic ensemble exemplified by our single photon creation scheme all rely on the atoms to keep the phase information imprinted on them by the collective scattering of a *Write* photon. As we have discussed before we can envision this process as the creation of a phased array of atoms. However atoms which are moving around will destroy this grating. If an atom is able to move half an optical wavelength it's phase information will be lost, and the collective enhancement into the cavity would be lost as well.

Assuming a simple Boltzmann distribution of atomic velocities, we will examine the scaling behavior with time that the recovery should follow. Starting with atom j at $\vec{x_j^0}$ when the *Write* photon is scattered the atom will be at a position $\vec{x_j} = x_j^0 + v_j t$ at a later time t. To examine the probability of recovery at time t we will just find the probability of overlap between the *Write* prepared state, $|L\rangle$, with the *Read* prepared state, $|E'\rangle$. Since we are only interested in seeing the scaling behavior we will combine normalization factors into A_n.

$$\begin{aligned}
|\langle L|E'\rangle|^2 &= \left| A_n \sum_{j=1}^{N} \cos\left(\vec{k_c}\cdot\vec{x_j}\right)\cos\left(\vec{k_c}\cdot\vec{x_j^0}\right) e^{-i\vec{k_w}\cdot\vec{x}_j^0} e^{i\vec{k_r}\cdot\vec{x}_j} \right|^2 \\
&= \left| A_n \sum_{j=1}^{N} \left[\cos^2\left(\vec{k_c}\cdot\vec{x_j^0}\right)\cos\left(\vec{k_c}\cdot\vec{v_j}t\right) - \frac{1}{2}\sin\left(\vec{k_c}\cdot\vec{x_j^0}\right)\right] e^{-i\vec{k_w}\cdot\left(2\vec{x_j^0}+\vec{v_j}t\right)} \right|^2
\end{aligned} \tag{4.4}$$

Taking the thermal average of Equation (4.4), defined as $\langle f(\vec{v})\rangle = \int_{-\infty}^{\infty} f(v) e^{-\frac{mv^2}{2kT}} d^3v$, we find that all the large terms follow a gaussian decay in time $e^{-\frac{t^2}{\tau_D^2}}$ where τ_D, known as the Doppler time, equals $\sqrt{\frac{m}{k_c^2 k_B T}}$.

The Doppler time is a measure of how long it takes to destroy the phase grating.

While our discussion has centered around the movement of atoms to destroy our superposition state, a much more abstract approach can be taken given that each atom is moving with velocity $\vec{v_j}$. In principle what created the massively symmetrized state was our inability to distinguish which atom scattered the original write photon. However if we were to study the photon for a long enough time to know it's frequency exactly, and how it differed from its original frequency we would know what Doppler shift had been incured by the moving atom. Furthermore if we knew this, we would be able to reconcile which atom did the scattering. This information perspective gives great insight into how we can vastly increase the doppler time. By confining an atom inside a deep potential well, we can limit the range of doppler shifts it can put on scattered photons [12]. This removes the ability to distinguish between the atoms in our grating by knowing their velocities. Therefore it seems quite obvious what our next step in creating our memory should be, further confining the atoms' motion.

4.3 Optical Lattices

While confining the motion of the atoms to localize them in space is the greatest concern which we hope to address, there are some key differences between what we want to accomplish with an Optical Lattice versus what was accomplished before with a MOT. In a MOT we relied upon the off-resonant scattering induced by the beams to both cool the atoms and localize them in space. For an Optical Lattice we will rely on light shifts which scale like $\frac{1}{\Delta}$. At this point in the experimental sequence, during the *Read* and *Write* processes, the atoms are already cooled and more likely than not, additional scattering will cause some residual heating which would in turn destroy the coherence of our shared excitation faster. Minimizing Raman scattering is quite simple as the scattering rate is proportional to $\frac{\Omega^2}{\Delta^2}$ and we can make the detuning Δ extremely large, minimizing scattering while still leaving an effect from light shifts to dominate the behavior of the system. To this end we use a commercially bought 1064 nm seed which we put through a 10 W fiber amplifier. But what forces do we have access to that do not involve scattering light that could be of use to us to trap

atoms?

The answer is a dipole interaction. While neutral atoms have no permanent electric dipoles, temporary dipole moments are induced in the atom in the presence of an electric field. In the dressed atom picture all the atoms have been cooled via PGC in state $|g\rangle$ and could absorb a photon to move to an excited state $|e\rangle$. Shown in Figure 4-4 the coupling between these levels change with beam intensity. Treating the system as a closed two level system and finding the energy spacing between the two new energy eigenstates we see they are separated by $\hbar\Omega(\vec{r})$ [10].

$$\begin{aligned}\hbar\Omega(\vec{r}) =& \hbar\sqrt{w(\vec{r})^2 + \Delta^2} \\ \approx& \hbar\Delta + \hbar\frac{w(\vec{r})^2}{2\Delta}\end{aligned} \tag{4.5}$$

Here $w(\vec{r})$ is the coupling constant between the two original levels and is proportional to the dipole interaction term: $|w(\vec{r})|^2 \propto \left|\vec{d}\cdot E(\vec{r})\right|^2$. This position dependent light shift pushes down the energy of the ground state exactly as the Stark effect would [30]. Due to the Optical Lattice's beam profile, the light shift is greatest at the center with a corresponding potential minimum. As we know that $F = -\frac{dU}{dr}$, the atoms will feel a force to localize at points of high beam intensity. This traps the atoms in the transverse direction of the beam. To create trapping along the longitudinal direction we retroreflect the beam to create a standing wave pattern, giving us a mostly one dimensional lattice.

To load the atoms into the lattice without causing an increase in kinetic energy from just slamming the lattice potential onto the atoms, as there is no guarantee that they won't get accelerated by these light shifts, a careful timing procedure has to be followed. While the procedures for loading a lattice with atoms can be very intricate, we instead follow a simple protocol [24]. We turn on the lattice during the polarization gradient cooling so that the scattering that takes place will load the atoms into the deepest parts of the lattice. The overlap between the PGC and optical lattice is a few ms, but that is all that is needed. With the lattice on we are able to hold the atoms in place when turning on our homogeneous magnetic field for 70

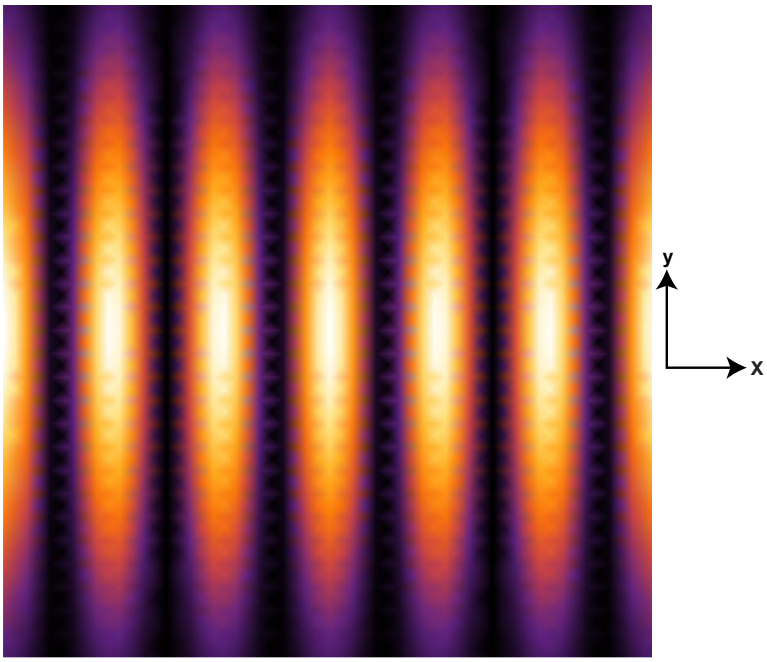

Figure 4-4: Plotted above is the 1D FORT (Far Off Resonance Trap) created with the retroreflection of a gaussian-like beam. Atoms will be attracted to the areas of high beam intensity. Due to the beams finite width in the y direction, there is an extremely small trap in the y direction. Interfering another beam is the only way to create strong trapping along any direction orthogonal to x.

ms, allowing all the stray fields induced by the eddy currents to die down. With the atoms fully prepared for implementing a quantum memory, we can begin discussing the final obstacles in our way and the results from the storage of photons from a weak coherent beam.

Chapter 5

Polarization Storage

To test our polarization storage we will compare the input state's polarization to the output state's polarization. This measure known as the Fidelity has a maximum value of $\frac{2}{3}$ when only classical means are used to store the polarization of the photon. Therefore all that needs to be accomplished is the polarization analysis on the output state to demonstrate a fidelity larger than the classical value of $\frac{2}{3}$. One complication remains however, as birefringence in all the optical elements through our make shift polarization analyzer on top of the chamber at the output of the cavity plus birefringence through the windows of the cavity introduce a rotation to the polarization we are trying to store and read out. As we will prove by correcting this rotation and examining representative states from different regions of the Poincaré sphere our quantum memory constitutes a reversible mapping between the state to be stored and the output of photon.

5.1 Fidelity of Stored Photons

On top of the chamber an array of waveplates and polarizing beam splitters have been placed such that we can analyze light in any of the three mutually orthogonal bases: Horizontal and Vertical (H-V), Left circularly polarized and Right circularly polarized (L-R), or $\pm\frac{\pi}{4}$ (S-T). Using polarizing beam cubes, we decompose the light in a manner that sends the two orthogonal states of the basis we are analyzing to

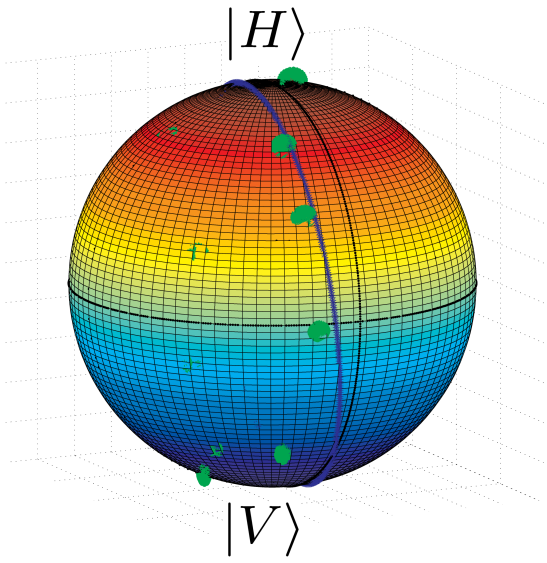

Figure 5-1: Plotted above is a representation of the Poincare sphere with horizontal and vertical polarization at the north and south pole, respectively. The green dots represent our data and the blue line represents the trajectory calculated from a preliminary measurement. We use the disagreement to the intended trajectory to calculate what rotation must be performed on the state to correct for stray birefringence in the system.

each SPCM separately. Therefore for repeated trials of any single input state we can in principle measure the output state's exact Stokes vector. When taking our final data on state to state mapping this will be the exact method we use. But we have yet to calculate the rotation the system puts on our input and output.

Rather than trying to analyze single points we will scan through a full great circle around the Poincaré sphere. This is easily accomplished, as to manipulate the *Write* beam to any conceivable polarization we placed a rotatable variable retarder and a $\frac{\lambda}{2}$ waveplate in the path of the beam. A variable retarder acts on the component of light polarized along its "slow" axis by adding a phase whose magnitude is controlled electronically by varying the amplitude of a square wave sent to the retarder. Scanning through a circle is simple as all one has to do is measure the recovery on each SPCM for a certain setting of all the waveplates and for a fixed value for the retarder voltage, and then change the voltage and repeat the measurement. Repeating this same sequence for each of the three bases we can measure interference fringes like in Figure 5-2.

Table 5.1: Fidelity Measurements for the Six Fiducial States.

Basis	H	V	L	R	S	T
p_{out}	0.85	0.86	0.90	0.96	0.85	0.85
F_{max}	0.93	0.93	0.95	0.98	0.93	0.92
F_{meas}	0.92(2)	0.92(2)	0.94(2)	0.98(1)	0.90(2)	0.92(2)

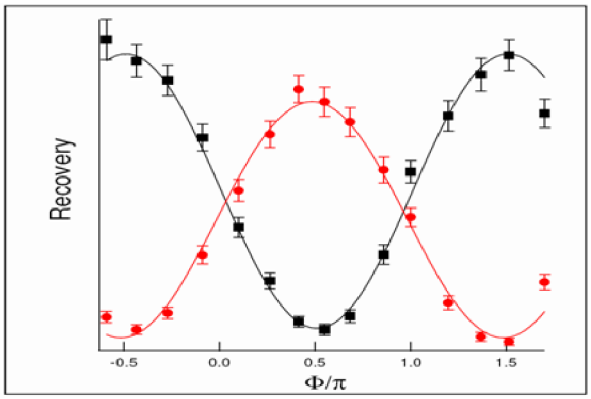

Figure 5-2: Plotted above is a representative interference fringe from two detectors seen when sweeping through one of the aforementioned great circle routes on the Poincare sphere.

Knowing the fringe visibility and the phase of the fringe in all three bases we are able to reconstruct which great circle we actually measured as can be seen in Figure 5-1.

The fidelity quoted in Table 5.1 is the overlap between the state we stored and the state we retrieved, which when the states are parametrized by Stokes vectors makes for a very simple analytic expression.

$$\begin{aligned}
F =& Tr\left[\rho_{\text{in}}\rho_{\text{out}}\right] \\
=& Tr\left[\frac{1}{4}\left(I+\vec{\sigma}\cdot\vec{S_{\text{in}}}\right)\left(I+\vec{\sigma}\cdot\vec{S_{\text{out}}}\right)\right] \\
=& Tr\left[\frac{1}{4}\left(I+\vec{\sigma}\cdot\left(\vec{S_{\text{in}}}+\vec{S_{\text{out}}}\right)+\left(\vec{\sigma}\cdot\vec{S_{\text{in}}}\right)\left(\vec{\sigma}\cdot\vec{S_{\text{out}}}\right)\right)\right] \\
=& Tr\left[\frac{1}{4}\left(I+\vec{\sigma}\cdot\left(\vec{S_{\text{in}}}+\vec{S_{\text{out}}}+\vec{S_{\text{in}}}\times\vec{S_{\text{out}}}\right)+I\left(\vec{S_{\text{in}}}\cdot\vec{S_{\text{out}}}\right)\right)\right] \\
=& \frac{1}{2}\left(1+\vec{S_{\text{in}}}\cdot\vec{S_{\text{out}}}\right)
\end{aligned} \tag{5.1}$$

The systematic rotation, between the input and the output states, was found

numerically using Jones Calculus. Relating the input state to the output state by some unknown rotation which we parametrize as a rotatable variable retarder followed by a $\frac{\lambda}{2}$ waveplate we perform a χ^2_ν minimization. The values that this procedure yields allow us to become reasonably close to correcting for the rotation. To characterize the quality of our memory we use the 6 fiducial states: H, V, L, R, S and T. At an average fidelity of 0.93(5) the system performs admirably well, with the greatest limitations caused by backgrounds [42]. Table 5.1 shows the measured fidelity, the length of the output stokes vector, and the maximum fidelity one could hope to achieve due to the output stokes vector magnitude being smaller than one. This change in stokes vector length is endemic from measuring so many background photons whose polarization is not the same as the photon that was stored. Comparing the measured fidelity with the maximum possible fidelity our reproduction of the polarization of the photon exhibits a high degree of accuracy.

Chapter 6

Conclusions

Did we cheat nature? By using a system of N atoms that is infinitly more complicated in its degrees of freedom compared to a single atom system, we have imposed quantum mechanics on a state which hedges on the macroscopic world. The benefits from this transition away from the microscopic to near macroscopic quantities allow a freedom of precision in the fundamental control of our Cesium atoms that is well within the realms of easily attainable modern technology. Exploiting the collective effects that allow us to store the photon's polarization and later create a single photon is not cheating nature but rather it is finding a loophole left open to us.

Even after all of this work, the greatest deficit of the system is in its decoherence time. To combat this instead of a 1D optical lattice a 2D optical lattice is being installed in the system for future experiments. But what can be done with this system even with long coherence times. The construction of a quantum memory inside a cavity lends itself to a large number of interesting experiments that probe the fundamentals of entanglement. Imagine for example that we were to find a way to increase our optical depth, or decrease our background rate to a point where we could send in a single photon, entangled in its polarization with another photon, instead of a weak coherent beam. How would the entanglement be transferred to the two magnons if at all and what would happen to the scattered *Write* photon remains an open question. Many such entanglement transfer experiments are possible. Looking forward however, it is not unreasonable to see the quantum memory as a tool for

many other quantum comunication experiments where it can act as a buffer along a communication pathway.

Bibliography

[1] Chad E. Bigelow, Nicusor V. Iftimia, R. Daniel Ferguson, Teoman E. Ustun, Benjamin Bloom, and Daniel X. Hammer. Compact multimodal adaptive-optics spectral-domain optical coherence tomography instrument for retinal imaging. *J. Opt. Soc. Am. A*, 24(5):1327–1336, 2007.

[2] K. M. Birnbaum, A. Boca, R. Miller, A. D. Boozer, T. E. Northup, and H. J. Kimble. Photon blockade in an optical cavity with one trapped atom. *Nature*, 436(7047):87–90, July 2005.

[3] Adam T. Black. *Collective Atom-Light Interactions Applied to Laser Cooling and Quantum Communication*. PhD thesis, Stanford University, 2005.

[4] Adam T. Black, James K. Thompson, and Vladan Vuletic. On-demand superradiant conversion of atomic spin gratings into single photons with high efficiency. *Physical Review Letters*, 95(13):133601, 2005.

[5] Eric D. Black. An introduction to pound–drever–hall laser frequency stabilization. *American Journal of Physics*, 69(1):79–87, 2001.

[6] Yu-Ao Chen, Shuai Chen, Zhen-Sheng Yuan, Bo Zhao, Chih-Sung Chuu, Jorg Schmiedmayer, and Jian-Wei Pan. Memory-built-in quantum teleportation with photonic and atomic qubits. *Nature Physics*, 4(2):103–107, February 2008.

[7] K. S. Choi, H. Deng, J. Laurat, and H. J. Kimble. Mapping photonic entanglement into and out of a quantum memory. *Nature*, 452(7183):67–71, March 2008.

[8] Class Notes from 8.322 Quantum Theory II at MIT in Spring 2007 with Prof. Robert Jaffe.

[9] Claude Cohen-Tannoudji, Jacques Dupont-Roc, and Gilbert Grynberg. *Atom Photon Interactions: Basic Processes and Applications*. John Wiley & Sons, Inc., New York, New York, 1992.

[10] J. Dalibard and C. Cohen-Tannoudji. Dressed-atom approach to atomic motion in laser light: the dipole force revisited. *J. Opt. Soc. Am. B*, 2(11):1707, 1985.

[11] J. Dalibard and C. Cohen-Tannoudji. Laser cooling below the doppler limit by polarization gradients: simple theoretical models. *J. Opt. Soc. Am. B*, 6(11):2023, 1989.

[12] R. H. Dicke. The effect of collisions upon the doppler width of spectral lines. *Phys. Rev.*, 89(2):472–473, Jan 1953.

[13] R. H. Dicke. Coherence in spontaneous radiation processes. *Phys. Rev.*, 93(1):99, Jan 1954.

[14] L.-M. Duan, M. D. Lukin, J. I. Cirac, and P. Zoller. Long-distance quantum communication with atomic ensembles and linear optics. *Nature*, 414(6862):413–418, November 2001.

[15] *Datasheet for Eaglyard Photonics DFB Laser: EYP-DFB-0852-00150-1500-T0C03-0000.*

[16] Christine Guerlin, Julien Bernu, Samuel Deleglise, Clement Sayrin, Sebastien Gleyzes, Stefan Kuhr, Michel Brune, Jean-Michel Raimond, and Serge Haroche. Progressive field-state collapse and quantum non-demolition photon counting. *Nature*, 448(7156):889–893, August 2007.

[17] William Happer. Optical pumping. *Rev. Mod. Phys.*, 44(2):169–249, Apr 1972.

[18] C. Henry. Theory of the linewidth of semiconductor lasers. *Quantum Electronics, IEEE Journal of*, 18(2):259–264, Feb 1982.

[19] Markus Hijlkema, Bernhard Weber, Holger P. Specht, Simon C. Webster, Axel Kuhn, and Gerhard Rempe. A single-photon server with just one atom. *Nature Physics*, 3(4):253–255, April 2007.

[20] Kees A. Schouhamer Immink, Ad. H. Hoogendijk, and Joost A. Kahlman. Digital audio modulation in the pal and ntsc laservision video disc coding formats. *Consumer Electronics, IEEE Transactions on*, CE-29(4):543–551, Nov. 1983.

[21] Brian Julsgaard, Jacob Sherson, J. Ignacio Cirac, Jaromir Fiurasek, and Eugene S. Polzik. Quantum state transfer and entanglement distribution among distant nodes in a quantum network. *Nature*, 432(7016):482–486, November 2004.

[22] Charles Kao and George A. Hockham. Dielectric-fibre surface waveguides for optical frequencies. *Proc. IEE*, 113:1151–1158, 1966.

[23] H. Kogelnik and C. V. Shank. Coupled-wave theory of distributed feedback lasers. *Journal of Applied Physics*, 43(5):2327–2335, 1972.

[24] S. J. M. Kuppens, K. L. Corwin, K. W. Miller, T. E. Chupp, and C. E. Wieman. Loading an optical dipole trap. *Phys. Rev. A*, 62(1):013406, Jun 2000.

[25] A. Kuzmich, A. D. Boozer, W. P. Bowen, A. Boca, C. W. Chou, L.-M. Duan, and H. J. Kimble. Generation of nonclassical photon pairs for scalable quantum communication with atomic ensembles. *Nature*, 423(6941):731–734, June 2003.

[26] Adam Lidz, Oliver Zahn, Matthew McQuinn, Matias Zaldarriaga, and Lars Hernquist. Detecting the rise and fall of 21 cm fluctuations with the murchison widefield array. *The Astrophysical Journal*, 680, Feb 2008.

[27] Huanqian Loh. Applications of correlated photon pairs: Sub-shot noise interferometry and entanglement. Bachelor's Thesis. Massachusetts Institute of Technology, June 2006.

[28] Rodney Loudon. *The Quantum Theory of Light*. Oxford Science Publications. Oxford University Press, Oxford, England, third edition, 2000.

[29] D. Maydan. Acoustooptical pulse modulators. *Quantum Electronics, IEEE Journal of*, 6(1):15–24, Jan 1970.

[30] J. D. Miller, R. A. Cline, and D. J. Heinzen. Far-off-resonance optical trapping of atoms. *Phys. Rev. A*, 47(6):R4567–R4570, Jun 1993.

[31] C. Monroe, W. Swann, H. Robinson, and C. Wieman. Very cold trapped atoms in a vapor cell. *Phys. Rev. Lett.*, 65(13):1571–1574, Sep 1990.

[32] New Focus, San Jose, CA. *Practical Uses and Applications of Electro-Optic Modulators*.

[33] E. M. Purcell. Spontaneous emission probabilities at radio frequencies. *Phys. Rev.*, 69(681), 1946.

[34] E. L. Raab, M. Prentiss, Alex Cable, Steven Chu, and D. E. Pritchard. Trapping of neutral sodium atoms with radiation pressure. *Phys. Rev. Lett.*, 59(23):2631–2634, Dec 1987.

[35] A. L. Schawlow and C. H. Townes. Infrared and optical masers. *Phys. Rev.*, 112(6):1940–1949, Dec 1958.

[36] U. Schünemann, H. Engler, R. Grimm, M. Weidemüller, and M. Zielonkowski. Simple scheme for tunable frequency offset locking of two lasers. *Review of Scientific Instruments*, 70(1):242–243, 1999.

[37] Marlan O. Scully and M. Suhail Zubairy. *Quantum Optics*. Cambridge University Press, Cambridge, UK, 1997.

[38] Anthony E. Siegman. *Lasers*. University Science Books, Mill Valley, CA, 1986.

[39] Jonathan Simon, Haruka Tanji, Saikat Ghosh, and Vladan Vuletic. Single-photon bus connecting spin-wave quantum memories. *Nature Physics*, 3(11):765–769, November 2007.

[40] Jonathan Simon, Haruka Tanji, James K. Thompson, and Vladan Vuletic. Interfacing collective atomic excitations and single photons. *Physical Review Letters*, 98(18):183601, 2007.

[41] Daniel A. Steck. Cesium d line data. Technical report, Los Alamos National Laboratory, 1998.

[42] Haruka Tanji, Saikat Ghosh, Jonathon Simon, Benjamin Bloom, and Vladan Vuletić. Single magnon quantum memory for photon polarization states. *Submitted for Publication to Nature Physics*, 2008.

[43] James K. Thompson, Jonathan Simon, Huanqian Loh, and Vladan Vuletic. A High-Brightness Source of Narrowband, Identical-Photon Pairs. *Science*, 313(5783):74–77, 2006.

[44] Wu-Ki Tung. *Group Theory in Physics*. World Scientific Publishing Co., Philadelphia, PA, 1985.

[45] Vladan Vuletić and Steven Chu. Laser cooling of atoms, ions, or molecules by coherent scattering. *Phys. Rev. Lett.*, 84(17):3787–3790, Apr 2000.

[46] Yifu Zhu, Daniel J. Gauthier, S. E. Morin, Qilin Wu, H. J. Carmichael, and T. W. Mossberg. Vacuum rabi splitting as a feature of linear-dispersion theory: Analysis and experimental observations. *Phys. Rev. Lett.*, 64(21):2499–2502, May 1990.